



Functional metabolomics characterizes the contribution of farnesoid X receptor in pyrrolizidine alkaloid-induced hepatic sinusoidal obstruction syndrome

Aizhen Xiong^{1,2} · Longhui Lu¹ · Kaiyuan Jiang¹ · Xiaoning Wang³ · Yan Chen¹ · Xunjiang Wang¹ · Wei Zhang⁴ · Yuzheng Zhuge⁴ · Wendong Huang⁵ · Lujin Li⁶ · Qi Liao¹ · Fan Yang⁷ · Ping Liu³ · Lili Ding^{1,2} · Zhengtao Wang^{1,2} · Li Yang^{1,2}

Received: 26 November 2023 / Accepted: 10 April 2024 / Published online: 4 May 2024
© The Author(s), under exclusive licence to Springer-Verlag GmbH Germany, part of Springer Nature 2024

Abstract

Consumption of herbal products containing pyrrolizidine alkaloids (PAs) is one of the major causes for hepatic sinusoidal obstruction syndrome (HSOS), a deadly liver disease. However, the crucial metabolic variation and biomarkers which can reflect these changes remain amphibious and thus to result in a lack of effective prevention, diagnosis and treatments against this disease. The aim of the study was to determine the impact of HSOS caused by PA exposure, and to translate metabolomics-derived biomarkers to the mechanism. In present study, cholic acid species (namely, cholic acid, taurine conjugated-cholic acid, and glycine conjugated-cholic acid) were identified as the candidate biomarkers (area under the ROC curve 0.968 [95% CI 0.908–0.994], sensitivity 83.87%, specificity 96.55%) for PA-HSOS using two independent cohorts of patients with PA-HSOS. The increased primary bile acid biosynthesis and decreased liver expression of farnesoid X receptor (FXR, which is known to inhibit bile acid biosynthesis in hepatocytes) were highlighted in PA-HSOS patients. Furtherly, a murine PA-HSOS model induced by senecionine (50 mg/kg, *p.o.*), a hepatotoxic PA, showed increased biosynthesis of cholic acid species via inhibition of hepatic FXR-SHP singling and treatment with the FXR agonist obeticholic acid restored the cholic acid species to the normal levels and protected mice from senecionine-induced HSOS. This work elucidates that increased levels of cholic acid species can serve as diagnostic biomarkers in PA-HSOS and targeting FXR may represent a therapeutic strategy for treating PA-HSOS in clinics.

Keywords Drug-induced liver injury · Cholic acid species · Farnesoid X receptor · Bile acid biosynthesis · Diagnosis marker · Potential therapy

✉ Aizhen Xiong
aizhenxiong@shutcm.edu.cn

✉ Lili Ding
nail8219@126.com

✉ Zhengtao Wang
ztwang@shutcm.edu.cn

✉ Li Yang
yl7@shutcm.edu.cn

¹ The MOE Key Laboratory for Standardization of Chinese Medicines and the SATCM Key Laboratory for New Resources and Quality Evaluation of Chinese Medicines, Institute of Chinese Materia Medica, Shanghai University of Traditional Chinese Medicine, Shanghai 201210, China

² Shanghai R & D Center for Standardization of Traditional Chinese Medicines, Shanghai 201210, China

³ E-Institute of Shanghai Municipal Education Committee, Institute of Interdisciplinary Integrative Medicine Research, Shanghai University of Traditional Chinese Medicine, Shanghai 201203, China

⁴ Department of Gastroenterology, The Drum Tower Hospital of Nanjing, Affiliated to Nanjing University Medical School, Nanjing 210008, Jiangsu, China

⁵ Department of Diabetes Complications and Metabolism, Diabetes and Metabolism Research Institute, Beckman Research Institute, City of Hope National Medical Center, Duarte, CA 91010, USA

⁶ Center for Drug of Clinical Research, Shanghai University of Traditional Chinese Medicine, Shanghai 201210, China

⁷ Department of Obstetrics and Gynecology, and Shanghai Key Laboratory of Gynecologic Oncology Ren Ji Hospital, Shanghai Jiao Tong University School of Medicine, Shanghai 200127, China

Abbreviations

CA	Cholic acid
CYP7A1	Cholesterol 7- α -hydroxylase
CYP8B1	Sterol 12- α -hydroxylase
FXR	Farnesoid X receptor
GCA	Glycocholic acid
HSOS	Hepatic sinusoidal obstruction syndrome
HBV	Hepatitis B virus infections
PBC	Primary biliary cirrhosis
PA	Pyrrolizidine alkaloid
PPAs	Pyrrole-protein adducts
ROC	Receiver operating characteristic
SHP	Small heterodimer partner
TCA	Taurocholic acid
OCA	Obeticholic acid

Introduction

Drug-induced liver injury is a frequent cause of liver injury. It can mimic both acute and chronic forms of liver disease and often represents a diagnostic and therapeutic challenge for the treating physician (Chalasanani et al. 2021; Hoofnagle and Björnsson 2019). The diagnosis of DILI, especially HILI caused by the intake of herbal medicines and herbal dietary supplements, is challenging due to the lack of characteristic clinical features and specific tests. Hepatic sinusoidal obstruction syndrome (HSOS) was initially described in the 1920s and linked to the ingestion of herbs/plants containing pyrrolizidine alkaloids (PAs) (Willont and Robertson 1920). To date, over 15,000 HSOS cases by PA exposure via food, health supplements, or herbal medicine such as *Gynura japonica* have been reported worldwide (Zhu et al. 2021; IPCS 1988). And PA-HSOS is now regarded as an intrinsic drug-induced liver injury and a well-known, albeit rare life-threatening disease (Hoofnagle and Björnsson 2019; Wang et al. 2018).

Given the high mortality rate of severe PA-HSOS (over 80%), extensive efforts have been devoted to enabling its accurate and timely diagnosis. The Roussel Uclaf Causality Assessment Method (Danan and Bénichou 1993) is popular for the diagnosis of DILI, but is not specific enough for PA-HSOS. The pathological confirmation by liver biopsy is regarded as the golden criteria for inspecting HSOS following hematopoietic stem cell transplantation (HSCT-HSOS) (Mohty et al. 2016; Jones et al. 1987; McDonald et al. 1984) that were potentiated by the chemotherapy and radiation therapy used during preparation for transplantation. However, ascites has been detected in nearly all PA-HSOS patients; and percutaneous liver biopsy in case of ascites can cause of severe complications (e.g., intraperitoneal bleeding and liver rupture), which makes it difficult to perform a liver biopsy in patients with PA-HSOS (Zhuge et al. 2018).

Recently, the Nanjing criteria for PA-HSOS (Zhuge et al. 2019) was promulgated by the Chinese Society of Gastroenterology Committee of Hepatobiliary Disease, which includes a confirmed history of PA-containing plant use (or the detection of blood pyrrole-protein adducts [PPAs, metabolites of PAs, which was used for traceability diagnosis with PA-HSOS]), elevation of serum total bilirubin or abnormal laboratory liver tests. Therefore, a noninvasive biomarker for the timely and accurate diagnosis of PA-HSOS in the clinic would be welcomed.

As new biomarkers of DILI emerge via metabolomics, circulating bile acids have been increasingly investigated both in animal studies and human studies (Schadt et al. 2016; Aubrecht et al. 2013). Metabolomics studies have noted that bile acids were broadly altered in rats exposed to 13 diverse hepatotoxins which are known to cause DILI, including acetaminophen (APAP) (Yamazaki et al. 2013). Notably, not all the bile acids in the plasma are consistently elevated upon exposure to these hepatotoxins, suggesting that selected bile acids in circulation could be potentially used as biomarkers for DILI. Glycodeoxycholic acid, for example, was identified as a prognostic biomarker for APAP-induced DILI (Woolbright et al. 2014). More recently, Tian et al. (2021) found that increased serum level of taurocholic acid (TCA) was correlated with the severity and clinical resolution of DILI.

Bile acids are synthesized in the liver from cholesterol (Myant et al. 1977). In the hepatocytes of liver, CA, and CDCA, two primary bile acids are catalyzed from cholesterol in the classic pathway mainly catalyzed by cholesterol 7- α -hydroxylase (CYP7A1), which further conjugate with taurine or glycine, and then reach the intestine through the bile duct to form secondary bile acids (such as DCA and LCA) via microbial modifications in the gut by deconjugation, dehydrogenation, dihydroxylation, epimerization, etc. CYP7A1 (via the classic pathway) and CYP8B1 (via the alternative pathway) function in primary bile acid biosynthesis from cholesterol. And studies have shown that when bile acid levels reach extremely high levels, the enzyme activities of CYP7A1 and CYP8B1 are repressed by a nuclear receptor cascade involving farnesoid X receptor (FXR, *NRIH4*) and small heterodimer partner (SHP, *NROB2*), thereby suppressing the biosynthesis of bile acids in hepatocytes (Li-Hawkins et al. 2002). Our previous studies (Xiong et al. 2014 and 2019) has noted that PA exposure in rodents impaired bile acids homeostasis in a way quite different from those in DILI induced by other toxins and the hepatic expression of farnesoid X receptor (FXR, *BR1H4*), which is known to inhibit bile acid biosynthesis in hepatocytes, was decreased. Disturbed bile acid homeostasis has also been discovered in rodents and liver cells exposed to PAs (Waizenegger et al. 2021; Pang et al. 2021; Hessel-Pras et al. 2020). However, the results obtained in these studies do not allow adequate translation of bile acids as biomarkers for PA-HSOS. In

addition, whether targeting FXR may represent an unrecognized therapeutic intervention for PA-HSOS remains unknown.

The present study aimed to identify informative diagnostic biomarkers of PA-HSOS using a combination of non-targeted metabolomics and targeted analysis of bile acids in clinical samples from two cohorts of PA-HSOS patients and patients with other different etiologies of chronic liver diseases. We also explored modulation of FXR activity as a potential therapy using a murine HSOS model induced by exposure to the PA senecionine, a representative hepatotoxic PA present in *Gynura japonica* extracts. Flow diagram of the study is illustrated in Fig. 1. This study translates metabolomics-derived biomarkers to the mechanism and lays the scientific basis for the clinical treatment of PA-HSOS.

Materials and methods

Patients and controls

Human sera samples and data of patients with HSOS were obtained retrospectively from Drum Tower Hospital. The diagnosis was independently performed by two experienced hepatologists, according to the Nanjing criteria for PA-HSOS (Zhuge et al. 2019). Simply, patients with a consistent diagnosis were included in the study, and those with inconsistent diagnosis were excluded. All patients were with a definite history of intake of PA containing herbs/plants, or the detection of blood pyrrole-protein adducts (PPAs) (metabolites of PAs) (Table S1). Patients with two or more liver diseases, or PA-HSOS in combination with biliary diseases, as well as unknown cause of liver disease, were excluded. Finally, 60 PA-HSOS patients were consecutively

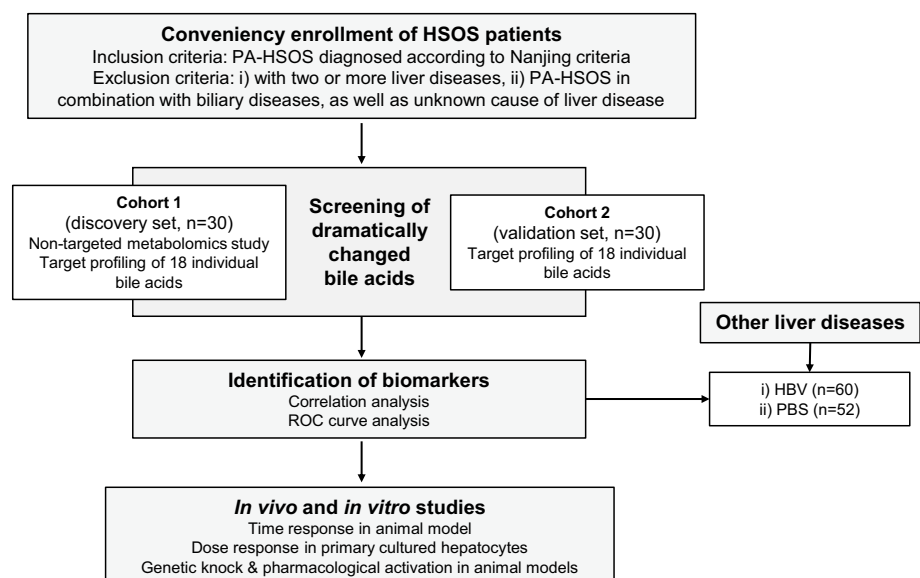
enrolled and were randomly divided into two cohorts: cohort 1 ($n=30$) for the discovery of potential biomarkers using non-targeted metabolomics approach and cohort 2 ($n=30$) for the validation of the biomarkers by targeted metabolic profiling. Age- and sex-matched healthy donors (HD, $n=30$) were recruited from subjects who participated in routine physical examinations at the same hospital. In addition, a total of 112 patients with different etiologies were enrolled in this study, including patients with hepatitis B virus infections (HBV, $n=60$) and primary biliary cirrhosis (PBC, $n=52$), from Shuguang Hospital. And the study was approved by the institutional review boards of corresponding hospitals and was designed and performed in accordance with the ethical guidelines of the 1975 Helsinki Declaration. The requirement for written informed consent was waived due to the retrospective nature of the study.

Chemicals and reagents

Senecionine with purity of over 98% was purchased from Chengdu Biopurify Phytochemicals, Ltd. (Sichuan, China) and dissolved in acidified 0.9% sodium chloride (pH 6.5) to prepare a solution containing 5 mg of senecionine per mL for animal experiments. Senecionine was also dissolved in acidified phosphate buffer to obtain a solution of 500 mM and diluted with culture medium for cell culture treatment. Obeticholic acid, the FXR agonist, with purity over 95% was purchased from AdipoGen Life Sciences (CA, USA) and suspended in 0.5% sodium carboxymethyl cellulose to prepare a mixture containing 2 mg of obeticholic acid per mL for animal experiments.

Authentic reference standards for bile acids were obtained from Sigma (NY, USA), including cholic acid (CA), taurine-conjugated CA (TCA), glycine-conjugated CA (GCA),

Fig. 1 Flow diagram of the study. Potential endogenous biomarkers for diagnosis of PA-HSOS were identified by using a combination of non-targeted metabolomics and targeted analysis of bile acids in clinical samples from two cohorts of PA-HSOS patients and patients with other different etiologies of chronic liver diseases. And the underlying mechanism was further explored using a murine HSOS model induced by senecionine, a representative hepatotoxic PA



chenodeoxycholic acid (CDCA), taurine-conjugated CDCA (TCDCa), glycine-conjugated CDCA (GCDCA), ursodeoxycholic acid (UDCA), taurine-conjugated UDCA (TUDCA), glycine-conjugated UDCA (GUDCA), hyodeoxycholic acid (HDCA), taurine-conjugated HDCA (THDCA), glycine-conjugated HDCA (GHDCA), deoxycholic acid (DCA), taurine-conjugated DCA (TDCA), glycine-conjugated DCA (GDCA), lithocholic acid (LCA), taurine-conjugated LCA (TLCA), glycine-conjugated LCA (GLCA), and D₄-CA (used as the internal standard in LC–MS analysis). FXR antibody (No. Ab85606) was purchased from Abcam (MA, USA).

Animal experiments

C57BL/6J mice were obtained from Laboratory Animal Services Centre, the Shanghai University of Traditional Chinese Medicine. FXR whole body knock-out (*Fxr*^{-/-}) mice (Ding et al. 2021) and the sibling littermates were obtained from the City of Hope National Medical Center. All mice were maintained on the standard laboratory by a 12 h light–dark cycle at 22 °C–25 °C and 55% ± 5% humidity-controlled environment with food and water ad libitum prior to the experiment. All animals were received humane care in compliance with regulations of experimental animal administration issued by the State Committee of Science and Technology of the People's Republic of China and the related ethics regulations of SHUTCM. All experiments were approved by the animal research committee of SHUTCM (Registration No. PZSHUTCM220808017). Prior to treatment, the mice were randomly divided into different groups, fasted overnight but with free access to water, and finally anesthetized with sodium pentobarbital for the collection of bio-samples.

An experimental HSOS model was established by exposing mice to senecionine at 50 mg/kg body weight (*p.o.*) according to our previous reports (Wang et al. 2022a, b; Yang et al. 2017). A cohort of male C57BL/6 J mice (8-week-old) were randomly divided into 4 groups with 13 mice each and then exposed to a single dose of 0.9% sodium chloride or senecionine (50 mg/kg body weight, *p.o.*) for 6, 12, 24, and 48 h. Ten mice from each group were anesthetized with sodium pentobarbital for the collection of blood samples, bile samples, liver tissues and ileum samples. Serum alanine aminotransferase (ALT) and aspartate aminotransferase (AST) activities, and total bilirubin (Tbil) and total bile acid (TBA) levels were determined with a Hitachi Automatic Analyzer 7080 (Hitachi High-Tech Science Systems Corp, Ibaraki, Japan). An aliquot of the liver tissues was applied for haematoxylin and eosin (HE) staining. The remaining three mice in each group were separately immobilized with glutaraldehyde through perfusion to prepare liver samples for scanning electron microscope (SEM) to identify

the ultrastructure of sinusoidal endothelium according our previous reports (Wang et al. 2022a, b).

To test the contribution of FXR in senecionine-induced toxicity, ten male *Fxr*^{-/-} mice (8-week-old) and the age- and sex-matched sibling littermates were randomly divided into two groups with five mice each and then exposed to a single dose of 0.9% sodium chloride or senecionine (50 mg/kg body weight, *p.o.*) for 24 h, respectively.

Obeticholic acid, the FXR agonist, was used to explore the potential therapy for PA-HSOS. HSOS mice (male C57BL/6 J mice, 8-week-old) induced by senecionine exposure (50 mg/kg body weight, *p.o.*) were either post-treated with obeticholic acid (20 mg/kg body weight, *p.o.*) at 6 and 30 h after senecionine exposure or pre-treated with obeticholic acid (20 mg/kg body weight, *p.o.*) for 3 days on a daily basis.

Primary hepatocytes culture and treatments

Murine hepatocytes were primary cultured according to the methods described previously (Yang et al. 2017). Cells were seeded into six well plates at the density of 2×10^5 in a 1 mL volume and then incubated with solvent control or serial concentrations of senecionine (2–20 μM) for 6 h for the collection of cell lysis.

Non-targeted metabolomics study

Sera samples from HD and PA-HSOS (cohort 1) was applied for a non-targeted metabolomics study by using previously reported UPLC-QTOF-MS approaches with minor modification (Beger et al. 2019; Zhang et al. 2018). Briefly, an aliquot of 100 μL of serum was precipitated by adding 400 μL of acetonitrile and methanol mixture (400 μL, v/v, 3:1) before being vortex for 10 s. Precipitated protein was then removed by centrifugation at 15,000 g for 10 min at 4 °C. And 400 μL of the supernatant was transferred to a tube and dried under a gentle stream of nitrogen at room temperature. Finally, the supernatant was reconstituted with 80 μL of water/acetonitrile (4:1) solution (containing 5 μg/mL L-2-chlorophenylalaine as the internal standard) for UPLC-QTOF-MS analysis. Besides, a control sample was made by mixing an aliquot of 5 μL of all serum samples and prepared by the method described above.

Chromatographic separation was performed on Waters ACQUITY UPLC BEH C18 column (2.1 × 100 mm, 1.7 μm) using Waters ACQUITY UPLC-QTOF-MS (Waters Corp., MA, USA). The column temperature was maintained at 45 °C. The gradient mobile phase condition was composed of phase A (5 mM ammonium acetate modified by the addition of 0.1% formic acid in waters) and phase B (acetonitrile), and the gradient elution was

as follows: 0–3 min, 10–40% B; 3–4 min, 40–60% B; 4–8.5 min, 60–65% B; 8.5–10 min, 65–95% B; 10–12 min, 95% B; 12–14 min, 95–10% B. The flow rate was 0.4 mL/min and the injection volume was 2 μ L. In addition, each sample was randomly analyzed thrice for technological repeat. The control sample was analyzed between every 20 samples to ensure the performance of the analysis.

The mass spectrometry and accurate mass acquisition was operated in both positive and negative modes with a waters QTOF Premier operating at electrospray ionization (ESI). The optimal capillary voltage was set at 3000 V, and cone voltage at 4 V. The source temperature was maintained at 120 °C, and the desolvation temperature (nitrogen) at 450 °C. The desolvation gas (nitrogen) flow rate was set at 800 L/h, and cone gas flow rate at 50 L/h, collision energy was set at 10 V to 30 V. Scan range was set from m/z 50–1000. During the MS analyses, all the data were collected using the lock spray to ensure accuracy and reproducibility. A lock-mass of leucine enkephalin (m/z 554.2615 in ESI- mode and m/z 556.2771 in ESI+ mode) was used for calculating the accurate molecular weight of biomarker candidates. The data were collected in centroid mode and the lock spray set at 10 s and averaged over 10 scans for correction.

Targeted quantification of bile acids

A total of 18 individual bile acids were quantified by using a previously described UPLC-MS method (Xiong et al. 2019; Yang et al. 2008) with standard curves prepared from authentic reference compounds.

Fluorescence immunostaining

Immunostaining of FXR was conducted on the liver tissues of humans, including patients with PA-induced HSOS ($n=3$) and patients without histologic liver injury (normal controls, NC) ($n=3$), which was acquired from diagnostic biopsy and surgical specimens and studied retrospectively. Human tissue materials were obtained from Nanjing Drum Tower Hospital, the Affiliated Hospital of Nanjing University School of Medicine (Jiangsu Province, China) in 2019. Signed informed consent was obtained from all participants prior to enrollment. This study was approved by the Ethics Committee of Nanjing Drum Tower Hospital and was designed and performed in accordance with the ethical guidelines of the 1975 Helsinki Declaration. All patients were diagnosed with PA-HSOS via consuming *G. japonica* in accordance with the previously described criteria (Zhuge et al. 2019).

qPCR

The total RNA of mouse primary hepatocytes or dissected liver and ileum tissues from mice was extracted using TRIzol Reagent (Invitrogen, TX, USA) in accordance with the manufacturer's protocol. cDNA was generated from 1 μ g of the total RNA with a PrimeScript® RT reagent kit incorporated with gDNA Eraser (Perfect Real Time) (Takara, Shiga, Japan). qPCR was performed using SYBR Premix Ex Taq (Takara, Shiga, Japan). Each sample was run in triplicate. The relative expression of each target gene was quantified using the $2^{-\Delta\Delta C_t}$ method and normalized to that of *Gapdh* using densitometry (Relative RNA expression = target gene/*Gapdh*). The primer sequences used for qPCR were listed in Table S2.

Molecular docking

A structure-based virtual screening was performed to test the effect of senecionine on FXR. The protein structure of FXR was downloaded from the protein data bank (PDB code: 4QE6). Molecular dynamics simulations were also performed to test the stability of the senecionine-FXR complex.

Luciferase assay

HEK293T cells were transfected with β RE (FXR downstream gene promoter region), expressed FXR and RXR α plasmids for 6 h using Lipofectamine 2000 (Invitrogen, Carlsbad, CA) (Yang et al., 2016). Then, the medium was replenished with fresh medium containing senecionine (5–100 μ M) and/or CDCA (100 μ M; a known FXR agonist) for 24 h. After treatment, cells were collected to measure firefly and renilla luciferase activity using the Dual-luciferase Reporter system (Promega, Madison, WI). Renilla luciferase activity was standardized to the Firefly luciferase activities.

Data analysis

The raw mass spectrometric data of UPLC-Q-Tof were analyzed using the MarkerLynx application manager for MassLynx 4.1 software (Waters Corp., MA, USA). The parameters were as follows: retention time range: 0–12 min; width of average peak at 5% height and peak-to-peak baseline noise were automatically calculated; no smoothing; marker intensity threshold: 2000 counts; mass window for marker collection: 0.02 Da; retention time window for marker collection: 0.1 min; noise elimination level: 6; isotopic peaks are removed for analysis. After data processing, a list of intensities of the peaks detected is generated using Rt (retention time) and m/z data pairs (Rt_ m/z) as identifiers for each peak. The corresponding ion intensities of each peak was normalized by the

internal standard (L-2-chlorophenylalaine), and the intensities in the three replicates of a same sample were averaged. Any peak with missing value (ion intensity = 0) in more than 20% samples or with variations over 30% in control sample was removed. The resulting matrix of each peak and corresponding ion intensity for each sample were further analyzed using SIMCAP software (Umetrics, Sweden).

The orthogonal projection to latent structure-discriminant analysis (OPLS-DA) was conducted to optimize model for screening the variables responsible for the discrimination of PA-HSOS patients from HD. The default seven-round cross-validation was used to guard against overfitting; 1/7th of the samples were excluded from the model in each round. And the R²Y(cum) and the Q²(cum) were calculated to estimate the goodness of fit of the model and the ability of prediction, respectively. Variable importance in the project (VIP) value and the OPLS-DA S-plot were used to identify the variables responsible for the differences between patients with PA-HSOS and HD, and markers were chosen based on their contribution to the variation and correlation with the data set.

Potential markers responsible for HSOS were identified by comparing their exact molecular masses, retention time, and MS/MS fragments data with the standard references available and those of data from literatures and online databases including Human Metabolome Database (<http://www.hmdb.ca/>), METLIN (<http://metlin.scripps.edu/index.php>), Lipid maps (<http://www.lipidmaps.org/>), KEGG (<http://www.genome.jp/kegg/>). And the pathway analysis of signatures revealed by metabolomics study was performed by the online MetaboAnalyst (<https://www.metaboanalyst.ca/>).

Indeterminate results of human samples were considered false-negative and incorporated into the final analysis. Missing values for clinical physical examinations (such as ALT, AST, etc.) were handled by the worst-case imputation. All quantitative data are presented as the mean \pm the standard error of mean (mean \pm SEM). Data were analyzed by the Student's *t*-test or one-way ANOVA analysis with LSD post hoc test using GraphPad Prism (Version 8; GraphPad, La Jolla, CA, USA). The bioinformatic analysis was conducted using R software (version 3.5.1; MathSoft, Seattle, WA). The difference in diagnostic performance was assessed using receiver operating characteristic (ROC) curves. And Spearman correlation analysis was performed. For all analysis, $p < 0.05$ was considered significant.

Results

Clinical characteristics of patients with PA-HSOS

Consumption of herbs/plants containing PAs, such as *G. japonica*, is a well-known factor for PA-HSOS in China (Zhu

et al. 2021; Zhuge et al. 2019). In the present study, physical examinations and a definite history of intake of PA containing herbs/plants or the detection of blood pyrrole-protein adducts (PPAs) (metabolites of PAs) based on UPLC-MS/MS analysis led to the diagnosis of 60 cases of PA-HSOS. Taking one 62-year-old male patient as an example: he took a decoction made from ~ 10 g of fresh-sliced *G. japonica* root on a daily basis for 1 month, and started to complain of abdominal distension for 16 days prior to being admitted to the Drum Tower Hospital (Jiangsu, China). In this case, the *G. japonica* herb was grown by the patient's family, and we were able to collect a sample and analyze it for PA contents. Approximately 3.89 mg of PAs per gram herb were detected in the herb sample, including 1.52 mg/g of senecionine and its *N*-oxide, 1.32 mg/mg of seneciphylline and its *N*-oxide, and 1.05 mg/g of seneciphyllinine and its *N*-oxide. The concentration of PPAs was 93.84 nmol/L in the serum of this patient. The severity of the disease was classified as very severe (score 4) according to the EBMT criteria for severity grading of HSCT-HSOS in adults promulgated by the European Society for Blood and Marrow Transplantation (Mohty et al. 2016). He was poorly responsive to supportive therapies such as anticoagulant treatment. And he improved after receiving trans-jugular intrahepatic portosystemic stent-shunt (TIPS) therapy.

The clinicopathological characteristics of the patients with PA-HSOS are summarized in Table 1. The average duration of the disease before patients were entered into the study was ~ 44 days (ranging from 5 to 135 days). Note that 67% of patients were classified as mild (score 1); 17% were classified as moderate (score 2); 3% were classified as severe (score 3); and 13% were classified as very severe (score 4). Given the present lack of known effective treatments for PA-HSOS in the clinic, patients commonly receive supportive therapies such as anticoagulant treatment (Zhuge et al. 2018 and 2019). However, those with more severe HSOS are unlikely to respond to anticoagulant treatment. There are reports of severe HSOS patients surviving after receiving TIPS therapy (Zhuge et al. 2019). In the present study, 40% of the patients were responsive to supportive therapies; 37% were poorly responsive to supportive therapies but improved after receiving TIPS therapy; 12% died; and the rate of follow-up loss was 12%.

PA-HSOS is associated with increased primary bile acids biosynthesis and elevated serum concentrations of cholic acid species

Firstly, a non-targeted metabolomics study was performed to identify potential biomarkers related to PA-HSOS (Fig. S1). OPLS-DA of the metabolomics data (analyzed using both positive and negative ion modes) revealed clear separation between the identified features present in the sera of HD

Table 1 Clinicopathological characteristics of patients with PA-HSOS

Characteristics	Cohort 1 (<i>n</i> = 30)		Cohort 2 (<i>n</i> = 30)	
	Mean	Incidence of abnormal (%)	Mean	Incidence of abnormal (%)
Age (y), mean (range)	62 (41,76)		64.5 (46,80)	
Male, <i>n</i> (%)	20 (67%)		20 (67%)	
Disease cause in days, mean (range)	54 (11–90)		47 (10–90)	
ALT (U/L), mean (range)	85.3 (17.1–317.2)	63.0	70.6 (12.4–281)	50.2
AST (U/L), mean (range)	110.6 (22.4–321.1)	81.5	81.1(22.6–381.7)	60.0
ALP (U/L), mean (range)	138.6 (53.2–380.1)	23.1	136.8 (75.3–244.4)	24.0
GT (U/L), mean (range)	137.3 (27–564)	84.6	118.1 (34–336.9)	88.0
Tbil (mmol/L), mean (range)	54.4 (8.7–360.9)	85.2	46.9 (16.9–239.3)	84.0
Dbil (mmol/L), mean (range)	39.7 (4.7–313.2)	96.2	27.3(6.9–137.5)	96.0
ALB (g/L), mean (range)	32.6 (29.1–37.6)	96.2	33.3 (27.1–49.4)	92.0
PT (s), mean (range)	15.1 (11.9–25.8)	48.0	25.5 (10.4–165.2)	56.5
DD (mg/mL), mean (range)	2.3 (0.27–9.43)	85.7	1.5 (0.2–6.15)	77.3
WBC (10 ⁹ /L), mean (range)	5.7 (3.07–11.1)	15.0	6.5 (3.5–11.8)	16.7
PL (10 ⁹ /L), mean (range)	122.5 (53–279)	52.4	106.4 (6.3–177)	66.7
PPAs (nmol/L), mean (range)	23.4 (0–80.16)	63.3	33.7 (0–190.4)	88.0
^a Severity grading, <i>n</i> (%)				
Mild (score 1)	19 (31.7)		21 (35.0)	
Moderate (score 2)	8 (13.3)		2 (3.3)	
Severe (score 3)	1 (1.7)		1 (1.7)	
Very severe (score 4)	2 (3.3)		6 (10.0)	
Survival outcome				
Responsive to supportive therapies	10 (16.7)		14 (25.0)	
Not responsive to supportive therapies but improved after receiving TIPS	12 (20.0)		10 (16.7)	
Death	2 (3.3)		5 (8.3)	
Follow-up loss	5 (8.3)		1 (1.7)	

Reference range: ALT, 6–40; AST, 6–40; ALP, 47–185; GT, 11–50; Tbil, 5–17.5; Dbil, 1.7–6.8; ALB, 35–50; PT, 10–15; D-Dimer, 0–0.5; WBC, 4–10; PL, 100–300; PPAs, 0

^aSeverity of the disease was classified according to the EBMT criteria for severity grading of HSCT-HSOS in adults. Abbreviation: HSOS, hepatic sinusoidal obstruction syndrome; ALT, alanine aminotransferase; AST, aspartate aminotransferase; ALP, alkaline phosphatase; GT, gamma glutamyl transpeptidase; Tbil, total bilirubin; Dbil, direct bilirubin; ALB, albumin; PT, Prothrombin time; DD, D-dimer; WBC, white blood cells; PL, platelets; PPAs, pyrrole-protein adducts (PAs metabolite)

and PA-HSOS (cohort 1) (Fig. 2A). With the aid of S-plots and VIP-plots, 49 differentially expressed endogenous compounds were identified (criteria: fold change > 1.5 and VIP value > 1.5) (Table S3). These compounds were predominantly bile acids, phosphatidylcholines (PCs), lysophosphatidylcholines (LysoPCs), sphingosine, amino acids, fatty acids, bilirubin, angiotensin, etc. Among them, bile acids, PCs, amino acids, bilirubin, and angiotensin were obviously increased in PA-HSOS patients. On the other hand, lysoPCs, fatty acids, and sphingosine were significantly decreased in PA-HSOS patients. These differentially expressed endogenous compounds were then used as input for pathway analysis. And several pathways were found to be significantly altered in PA-HSOS patients, including primary bile acids biosynthesis, fatty acid biosynthesis, sphingolipid

metabolism and alpha-linolenic acid metabolism. Most obviously, the pathway for primary bile acids biosynthesis was dramatically increased in patients with PA-HSOS (Fig. 2B), a finding consistent with results from our previous genomics and metabolomics study in rodents after senecionine exposure (Xiong et al. 2014). We then evaluated the protein level of FXR (known to inhibit the biosynthesis of primary bile acids in hepatocytes) in liver tissues from diagnostic biopsies and surgical specimens of PA-HSOS patients (*n* = 3) and NC (*n* = 3) by fluorescence immunostaining. FXR levels were obviously decreased in livers of patients with PA-HSOS compared to NC (Fig. 2C).

We then quantified the 18 bile acids (including 6 primary bile acids and 12 secondary bile acids) in sera samples from HD and PA-HSOS (cohort 1 and 2) and found

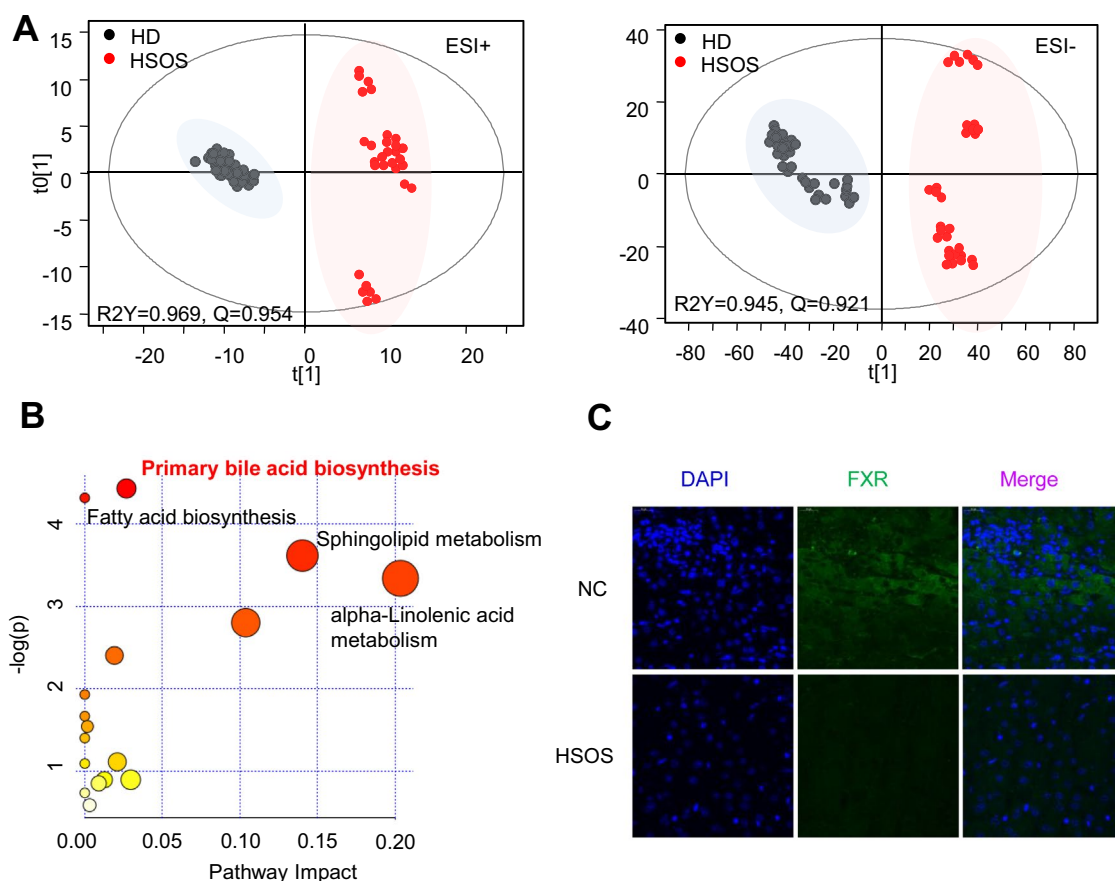


Fig. 2 PA-HSOS is associated with increased serum concentrations of cholic acid species and decreased FXR in liver tissues. OPLS-DA score plots (**A**) and Pathway analysis of signatures from the non-targeted metabolomics dataset (**B**). **C** Typical fluorescence immunostaining image of FXR in liver tissues from patients of PA-HSOS ($n=3$) and NC ($n=3$)

several individual bile acids were dramatically increased in the patients with PA-HSOS (Fig. 3A). Among them, CA, TCA and GCA were increased by 14.5 to 96.9-fold (CA: 0.50 nmol/ml serum in HD vs 7.25 nmol/ml serum in Cohort 1 and 7.78 nmol/ml serum in Cohort 2; TCA: 0.15 nmol/ml serum in HD vs 14.54 nmol/ml serum in Cohort 1 and 5.13 nmol/ml serum in Cohort 2; GCA: 0.79 nmol/ml serum in HD vs 36.89 in Cohort 1 and 21.74 nmol/ml serum in Cohort 2), respectively. We then compared different bile acid species as concatenated into various groups (including for example unconjugated and conjugated bile acids) and noted especially dramatic elevation of CA species (fold change = 40.6, $p < 0.001$) (Fig. 3B and Fig. 3C); the term cholic acid species (CA species) here refers to CA, TCA, and GCA. Moderately elevated serum Tbil is common for most patients with PA-HSOS (Zhang et al. 2021) and a significant difference in serum Tbil between those PA-HSOS patients who survived and those who died during a follow-up period of 3 years was reported (34.3 versus 44.0 $\mu\text{mol/L}$, $p < 0.05$) (Shang et al. 2021). Spearman correlation analysis showed that total and individual CA species were positively

correlated with Tbil levels in patients with PA-HSOS (Fig. S2A and S2B). ROC analyses suggested that CA species have potential diagnosis capacity for PA-HSOS (AUC 0.968 [95% CI 0.908–0.994], sensitivity 83.87%, specificity 96.55%) with a cut-off value of 1.5 $\mu\text{mol/L}$ (Fig. 2D and Table S4). Interestingly, the level of CA species was significantly increased in the PA-HSOS patients who were not responsive to supportive therapies as compared to those who were responsive to supportive therapies (81.5 versus 21.9 $\mu\text{mol/L}$, $p < 0.01$; AUC 0.745 [95% CI 0.597–0.861], sensitivity 68.18%, specificity 76.00%, $p < 0.001$) with a cutoff value of 26.2 $\mu\text{mol/L}$ (Fig. S3), implying a good ability in differentiating those PA-HSOS patients likely to be responsive to therapy.

PPAs (the currently recommended xenobiotic markers for PA-HSOS, whose exact structures are largely unknown) were detected in 72% of patients with PA-HSOS (Table 1) and poorly correlated with Tbil ($r = -0.11$, $p = 0.49$). PPAs are with highly specificity for diagnosing PA-HSOS from HD (specificity 100.00%) yet with low sensitivity (70.97%) (Fig. S4A and B); PPAs levels are poorly correlated with

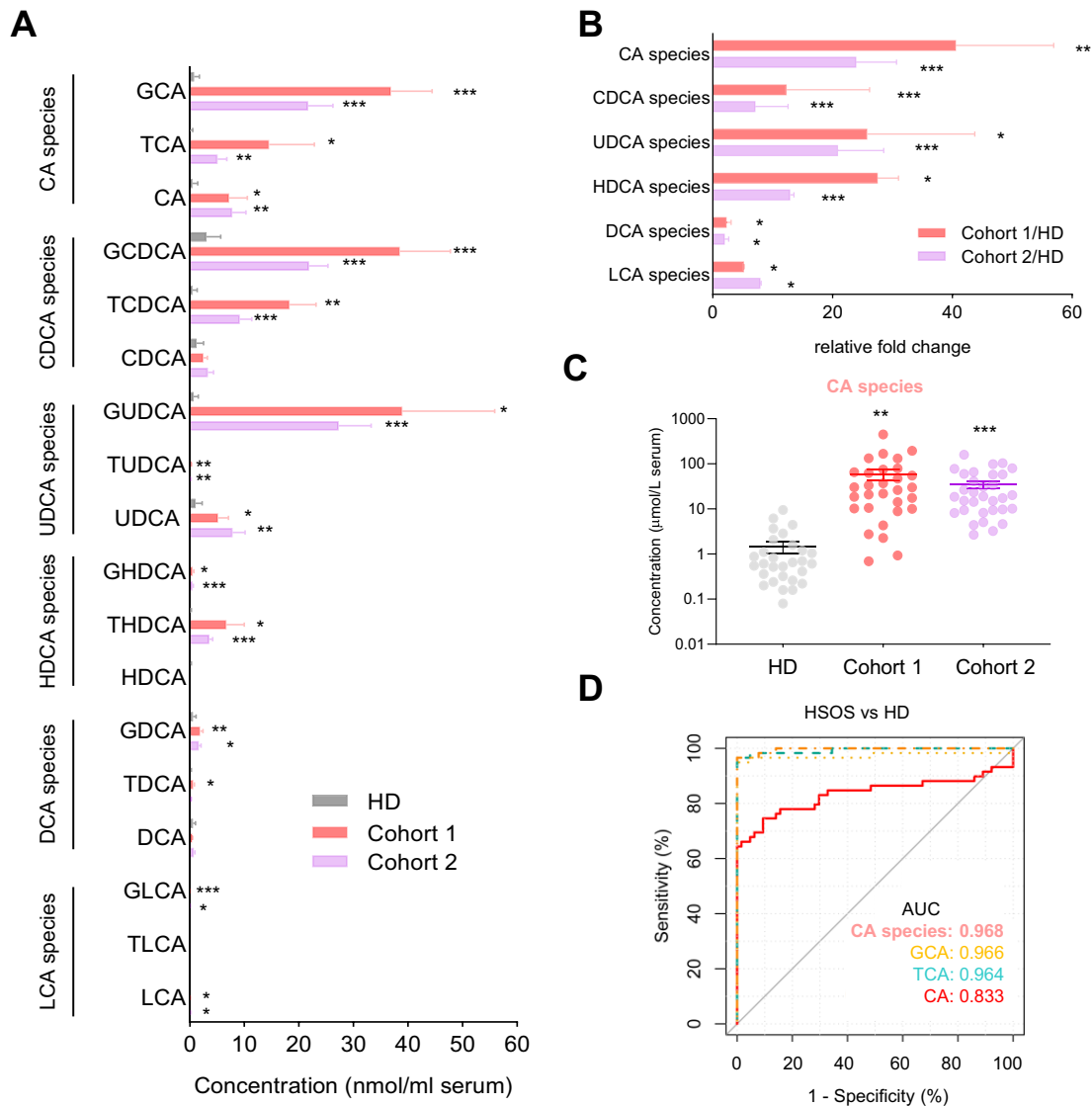


Fig. 3 PA-HSOS is associated with increased serum concentrations of cholic acid species. **A** Contents of 18 individual bile acid in PA-HSOS patients. **B** Fold change of 6 bile acid species in PA-HSOS patients relative to the mean values of healthy controls. Concentration **C** and diagnostic performance of CA species in differentiating patients with PA-HSOS from HD **D**. Values are expressed as the mean \pm SEM. ** $p < 0.01$, *** $p < 0.001$ vs. HD. CA, cholic acid; GCA, glycocholic acid; TCA, taurocholic acid; CDCA, chenodeoxy-

cholic acid; GCDCA, glycochenodeoxycholic acid; TCDC, taurochenodeoxycholic acid; UDCA, ursodeoxycholic acid; GUDCA, glycooursodeoxycholic acid; TUDCA, taurooursodeoxycholic acid; HDCA, hyodeoxycholic acid; GHDCA, glycohyodeoxycholic acid; THDCA, taurohyodeoxycholic acid; DCA, deoxycholic acid; GDCA, glycodeoxycholic acid; TDCA, taurodeoxycholic acid; LCA, lithocholic acid; GLCA, glycolithocholic acid; TLCA, tauroolithocholic acid

the severity of the disease (AUC 0.587, sensitivity 54.55%, specificity 72.00%, $p = 0.305$) (Fig. S4C and D). PPAs are a specific but not a sensitive indicator for PA-HSOS diagnosis. Taken together, CA species apparently outperform PPAs for diagnosing PA-HSOS.

Elevation of serum bile acids in different etiologies of chronic liver diseases (HBV, PBC, etc.) have also been reported (Wei et al. 2023; Sang et al. 2021; Chen et al. 2020a, b). Thus, the specificity of CA species for PA-HSOS

was also determined in present study. Compared with patients with other etiologies in liver injury, PA-HSOS patients had obviously higher concentration of total CA species, GCA, TCA, and CA (Fig. S5A) and the three etiologies showed different patterns in CA species (Fig. S5B). ROC analyses showed that AUCs for total CA species were 0.759 (95% CI 0.673–0.845; sensitivity 81.36%, specificity 63.33%) in PA-HSOS patients and HBV patients (Fig. S5C), and 0.757 (95% CI 0.669–0.846; sensitivity 81.36%,

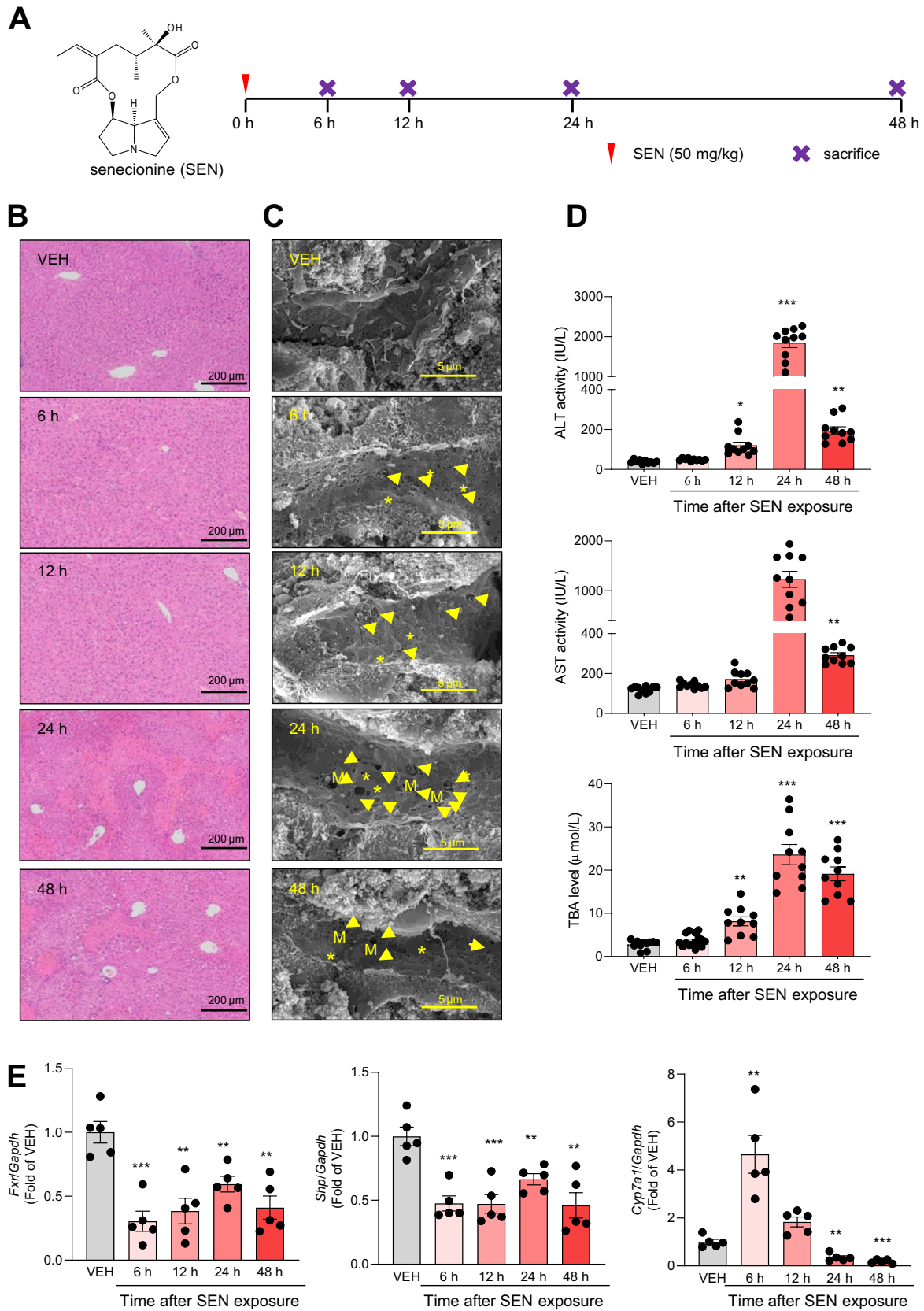


Fig. 4 Senecionine induces severe liver injury in mice. Mice were orally treated with blank solvent (VEH) or senecionine (SEN, 50 mg/kg) for 6, 12, 24 and 48 h. **A** Typical images of HE staining of liver tissues ($n=3$). Scale bar: 200 μm . **B** Typical scanning electron microscopy images of liver tissues ($n=3$). Scale bar: 5 μm . The yellow asterisk indicates the loss of fenestrae organized as sieve plates in sinusoidal. The yellow arrow indicates the formation of large gaps in the sinusoidal endothelium and exposure of the Disse space. M indicates the visible hepatocyte microvilli through the gap in HSECs. **C** Serum ALT and AST activities, and TBA levels ($n=10$). **D** The hepatic mRNA expression of *Fxr*, *Shp*, and *Cyp7a1* ($n=5$). Values are expressed as the mean \pm SEM. * $p < 0.05$, ** $p < 0.01$, *** $p < 0.001$ vs. VEH group

specificity 59.61%) in PA-HSOS patients and PBC patients, respectively (Fig. S5D), suggesting that CA species levels have potential capacity for distinguishing PA-HSOS from HBV and PBC.

Senecionine induces severe HSOS in murine and inhibits hepatic FXR

Experimental HSOS models have been well established by oral exposure to monocrotaline (Huang et al. 2019; DeLeve et al. 1999), senecionine (Hessel-Pras et al. 2020; Yang et al. 2017; Lin et al. 2011), or retronecine (Wang et al. 2022a, b; He et al. 2021). In the last decades, PA-HSOS cases are often associated with the oral intake of *G. japonica* (Zhu et al. 2021; Zhuge et al. 2019), in which senecionine is identified as one of the major PAs (Wang et al. 2022a, b; Xiong et al. 2019; Lin et al. 2011). Therefore, we here induced a previously reported murine HSOS model by a single oral exposure of senecionine.

Senecionine exposure (50 mg/kg) caused the loss of fenestrae in the hepatic sinusoidal endothelium of mice and large gaps in the sinusoidal endothelium at 6 h after senecionine treatment and more severe injury occurs at 12–48 h after senecionine treatment (Fig. 4). Notably, senecionine exposure for 24 h showed the most severe hepatic parenchymal cell injury and sinusoidal endothelium damage (Fig. 4B and C), which was typical for PA-HSOS. Serum ALT and AST activities were peaked at 24 h after senecionine exposure and decreased greatly at 48 h after senecionine exposure while TBA levels were kept at high level at 24–48 h after senecionine exposure (Fig. 4D). In addition, hepatic mRNA expression of *Fxr* was decreased after senecionine exposure (Fig. 4E), which was consistent with the decreased hepatic expression of FXR in PA-HSOS patients. A nuclear receptor cascade involving FXR and SHP is reported to suppress the activity of CYP7A1 and CYP8B1 thus suppressing bile acid biosynthesis in liver and contributing to bile acid homeostasis (Russell 2003; Chiang 2003; Myant and Mitropoulos 1977). qPCR analysis of the dissected liver tissue from HSOS model mice showed significant decrease in the mRNA levels of *Fxr* (Fig. 4E). Further, senecionine exposure

also resulted in decreased hepatic mRNA levels of *Shp* yet increased *Cyp7a1* level, supporting that senecionine exposure affects FXR's down-stream genes in mice.

Elevated serum concentrations of cholic acid species are detected in a murine HSOS model induced by senecionine

Individual bile acids were then quantified in samples from mice with senecionine exposure for 24 h. As noted, several individual bile acids were elevated in mice exposed to senecionine for 24 h (Fig. 5A). Among them, CA was increased by 5.9-fold (0.16 nmol/ml serum in VEH vs 0.95 nmol/ml serum in SEN), TCA increased by 31.4-fold (0.27 nmol/ml serum in VEH vs 8.48 nmol/ml serum in SEN), and GCA increased by 20.0-fold (0.01 nmol/ml serum in VEH vs 0.02 nmol/ml serum in SEN), respectively. And all bile acid species were obviously increased, among which CA species showed especially dramatic elevation (about 21.7-fold, 0.44 nmol/ml serum in VEH vs 9.45 nmol/ml serum in SEN) (Fig. 5B). This phenomenon was consistent with our findings for the PA-HSOS patients in present study. We collected bile flow and dissected liver and ileum samples from naïve control and senecionine-induced HSOS model mice (senecionine exposure for 24 h) to assess potential impairment of CA species (Fig. S6). Compared to controls, the level of CA species was increased by 82% in the liver yet was decreased by 34% in bile flow from the HSOS model animals; this level did not change in the ileum (Fig. 5C); individually, the TCA level increased by 54% in the liver yet was decreased by 33% in bile flow, and the CA level was increased by 308% in the liver yet was decreased by 66% in bile flow and by 72% in the ileum samples (Fig. S6). These data suggest an increased accumulation of CA species in liver and decreased secretion of CA species in bile flow and ileum. qPCR analysis of the dissected liver tissue from HSOS model mice showed significant decrease in the mRNA levels of *Fxr* (Fig. 5D). Further, senecionine exposure also altered the hepatic mRNA levels of *Fxr* downstream genes responsible for bile acids biosynthesis (i.e., *Shp*, *Cyp7a1* and *Cyp7a1*) and secretion including multidrug resistance-associate protein 2 (*Mrp2*) and the bile salt export pump (*Bsep*).

The inhibition effect of senecionine on FXR were also evaluated by in silico and in vitro studies. First of all, molecular docking was performed (Fig. 5E). The docking score showed that the binding force of senecionine with FXR was -10.279 kcal/mol (while the positive drug obeticholic acid was -14.916 kcal/mol). The senecionine-FXR complex was further analyzed by molecular dynamics simulation at 100 ns (Fig. S7). The RMSD of the complex is between 0.15 and 0.25 and the RMSD fluctuation is rather small, indicating that the senecionine-FXR complex is stable. According to the analysis of centroid evolution (Fig.

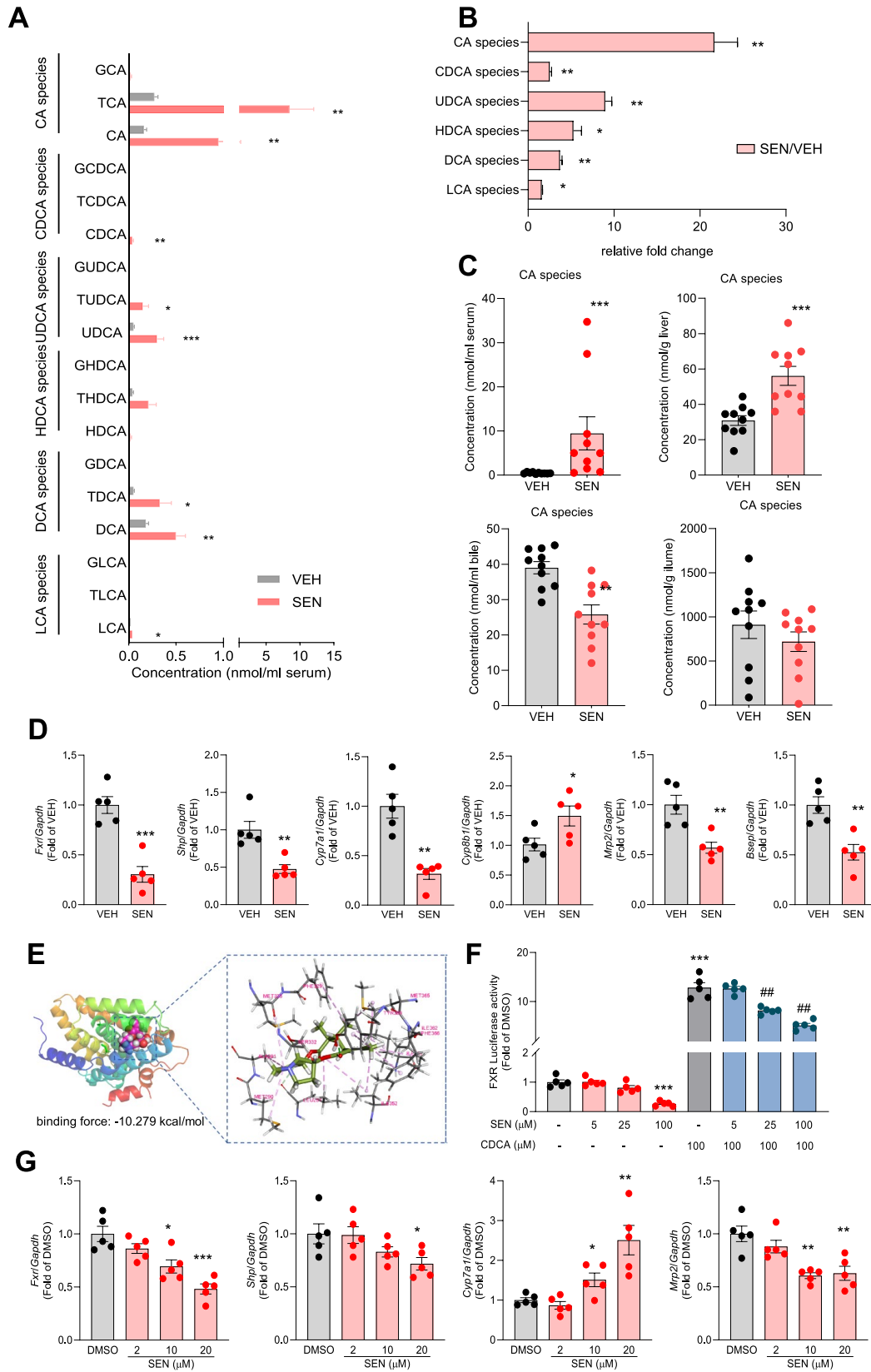


Fig. 5 Increased serum concentrations of cholic acid species are detected in a murine HSOS model induced by senecionine. A murine HSOS model was established based on a single exposure to senecionine (50 mg/kg) orally for 24 h. **A** Concentration of individual bile acid in serum. **B** Changes of 6 bile acid species in HSOS mice. **C** Concentration of CA species in serum, liver, bile and ileum samples. **D** The mRNA expression of *Fxr* and downstream genes in dissected liver tissues. **E** The binding mode of senecionine to FXR receptor. **F** Effect of senecionine on FXR luciferase activity in primary cultured murine hepatocytes. **G** The mRNA expression of *Fxr* and downstream genes in primary cultured murine hepatocytes after senecionine exposure. Values are expressed as the mean \pm SEM. * $p < 0.05$, ** $p < 0.01$, *** $p < 0.001$ vs. VEH group. ## $p < 0.01$, ### $p < 0.001$ vs. CDCA treatment

S7B), senecionine in the complex is always located at the initial binding site of the protein and the distance between senecionine and FXR protein and the initial binding site in senecionine-FXR complex is very stable. The binding energy decomposition analysis showed (Table. S5) that van der Waals force played a major role in senecionine-FXR complex, and electrostatic interaction and hydrophobic interaction played a complementary role. The binding energy of senecionine-FXR complex was -127.031 kJ/mol. These data proved that senecionine shows high potency of binding with FXR. Then Luciferase analysis was performed to test whether senecionine impaired bile acids homeostasis through modulating FXR activity. As results, senecionine significantly inhibited FXR in a dose-dependent manner with or without FXR activation by CDCA, a known FXR agonist (Fig. 5F). Additionally, effects of senecionine on the mRNA expression of FXR down-stream genes were also investigated in mice primary cultured hepatocytes. Senecionine exposure significantly decreased the mRNA expression levels of *Fxr*, *Shp*, and *Mrp2* while increased the mRNA expression level of *Cyp7a1* (Fig. 5G), suggesting an increase in bile acid biosynthesis in hepatocytes.

On the other hand, no obvious changes between naïve controls and HSOS model mice were found in the ileum for the mRNA expression of *Fxr* or its known downstream genes such as fibroblast growth factor 15 (*Fgf15*), ileum bile acid-binding protein (*Ibabp*), etc. (Fig. S8). The data indicated that senecionine exposure inhibited hepatic FXR-SHP signaling, which then increased bile acid biosynthesis in liver. Therefore, activating FXR might be a new therapy for PA- HSOS in clinics.

The FXR agonist obeticholic acid protects mice from senecionine-induced HSOS

Considering the importance of FXR in senecionine-induced toxicity, *Fxr*^{-/-} mice were exposed to senecionine. We noted that the extent of senecionine-induced liver injury is exacerbated in *Fxr*^{-/-} HSOS model mice, as assessed based on histological changes and serum indexes (Fig. 6). FXR

deficiency can lead to cholestasis (Wang et al. 2008), and *Fxr*^{-/-} mice are highly sensitive to liver injuries induced by hepatotoxins such as APAP (Yan et al. 2021; Lee et al. 2010). *Fxr*^{-/-} mice develop spontaneous liver tumors with aging (Yang et al. 2007). Recently, FXR deficiency is found to potentiate iron hepatotoxicity, accompanied with hepatic steatosis as well as dysregulated iron and bile acid homeostasis (Xiong et al. 2022). These lines of evidence imply that FXR may protect mice against senecionine-induced HSOS.

OCA is a known FXR agonist (Pellicciari et al. 2002) and is FDA-approved for treatment of primary biliary cholangitis patients not responding or intolerant to UDCA (Nevens et al. 2016). We used OCA to test whether pharmacological activation of FXR can protect mice from senecionine-induced HSOS. Histologically, OCA treatment at 6 and 30 h after senecionine exposure attenuated senecionine-induced HSOS (Fig. 7). The magnitude of increase in serum ALT and AST activities and Tbil and TBA levels was also decreased in mice that were treated with OCA after senecionine exposure (Fig. 7C). In addition, the magnitude of the increase in CA species in dissected liver tissues was reduced by OCA treatment (Fig. 7D) and the magnitude of the changes in the mRNA expression of *Fxr*, *Shp* and *Cyp7a1* in dissected liver tissues was recovered by OCA treatment (Fig. 7E). We also pretreated mice with OCA for 3 days before senecionine exposure to test if there is any prophylactic effect from this FXR agonist. The extent of senecionine-induced hepatic parenchymal cell injury and the damage in the sinusoidal endothelium (evident by loss of fenestration on the sieve plate) was reduced in mice that were pretreated with OCA prior to model induction (Fig. 8). The serum levels of CA species as well as altered mRNA expression of *Fxr* and int downstream genes were also recovered to normal in HSOS model mice pretreated with OCA. These results demonstrate that activation of FXR with the agonist OCA can confer therapeutic effects against senecionine-induced HSOS in mice.

Discussion

Diagnosing PA-HSOS is difficult because the manifestations in PA-HSOS overlap with other liver diseases (Zhang et al. 2021; Zhuge et al. 2019). This will result in a lack of effective prevention, diagnosis and treatments against this disease. The pathological confirmation by liver biopsy is regarded as the gold standard for diagnosing HSOS. However, it is difficult to perform a liver biopsy in patients with PA-HSOS because percutaneous liver biopsy in case of ascites can cause of severe complications (e.g., intraperitoneal bleeding and liver rupture). As a continuation of our investigation into the toxicity and safety assessment of PA-containing herbs, our present study examined candidate

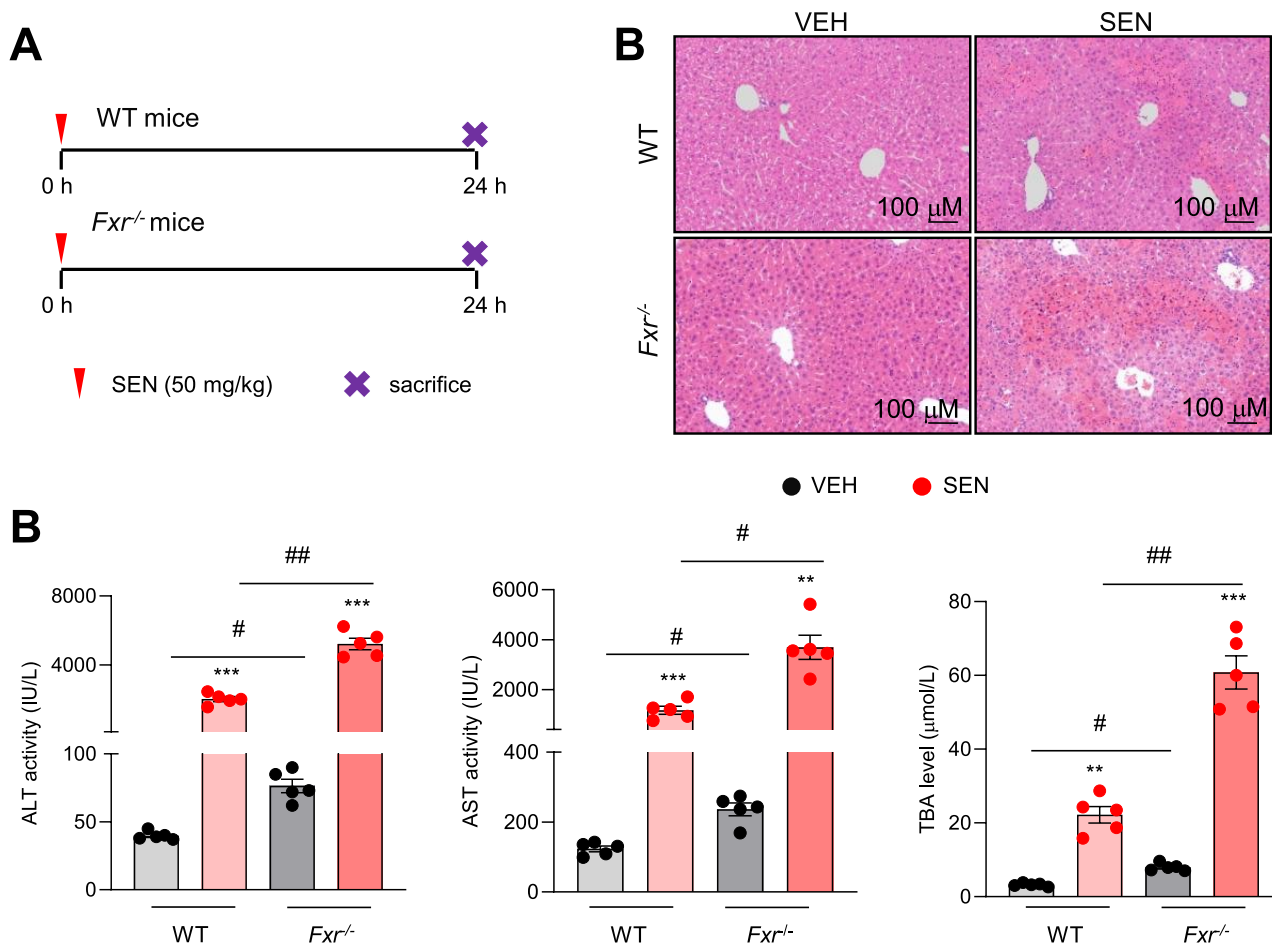


Fig. 6 *Fxr*^{-/-} aggregates senecionine-induced HSOS in mice. **A** *Fxr*^{-/-} mice and WT mice were orally treated with senecionine (50 mg/kg) for 24 h. **B** HE staining of liver sections. **C** Serum levels of ALT,

AST, and TBA. Values are expressed as the mean ± SEM. ***p* < 0.01, ****p* < 0.001 vs. VEH between mice in same genotypes. #*p* < 0.05, ##*p* < 0.01 vs. mice received same treatment

endogenous biomarkers for the diagnosis of PA-HSOS by using UPLC-MS based metabolomic approaches with clinical samples from patients with PA-HSOS, and efforts had been made to translate metabolomics-derived biomarkers to the mechanism. Our major findings were as follows: (1) primary bile acid biosynthesis was dramatically increased in patients with PA-HSOS; (2) increased CA species (CA, TCA, and GCA) are potential diagnostic markers for PA-HSOS; (3) FXR agonist obeticholic acid reduced CA species to normal levels in senecionine-induced HSOS model mice and protected mice from senecionine-induced HSOS (Fig. 9).

PPAs have been identified as metabolite biomarkers for PA-HSOS (Zhuge et al. 2019; Gao et al. 2015); however, analysis of the 60 PA-HSOS patients in the present study shows that PPAs content varied from undetected to hundreds of nmol/L in serum. Gao et al. (2015) also established that variance PPAs content is linked to both the amount and the duration of PA intake, as well as on sampling time. Our

previous kinetic study of PPAs in an experimental HSOS model caused by multiple exposure of mice to *G. japonica* extracts study proved that PPAs cleared faster in serum ($T_{1/2ke} \sim 4.0$ days) and more than 90% PPAs were removed 2 weeks after the last dosing (Chen et al. 2020a, b). However, lots of patients have no awareness of PA exposure and it usually takes weeks to months for the onset of PA-HSOS (Zhuge et al. 2019). Thus, and as noted previously, PPAs are suitable for traceability diagnosis with PA-HSOS in the newly promulgated Nanjing criteria for PA-HSOS (Zhuge et al. 2019). Furthermore, the simplified Nanjing criteria, in which the detection of blood PPAs and the history of ingesting PA-containing herbal medicine/plants were not included, also exhibit excellent performance in diagnosing PA-HSOS (Zhang et al. 2021).

Previous studies have revealed increased serum level of total bile acids in animals exposed to PAs (Sutherland et al. 1992; Mendel et al. 1988). These results suggested that total bile acids in serum could be a sensitive index of hepatic

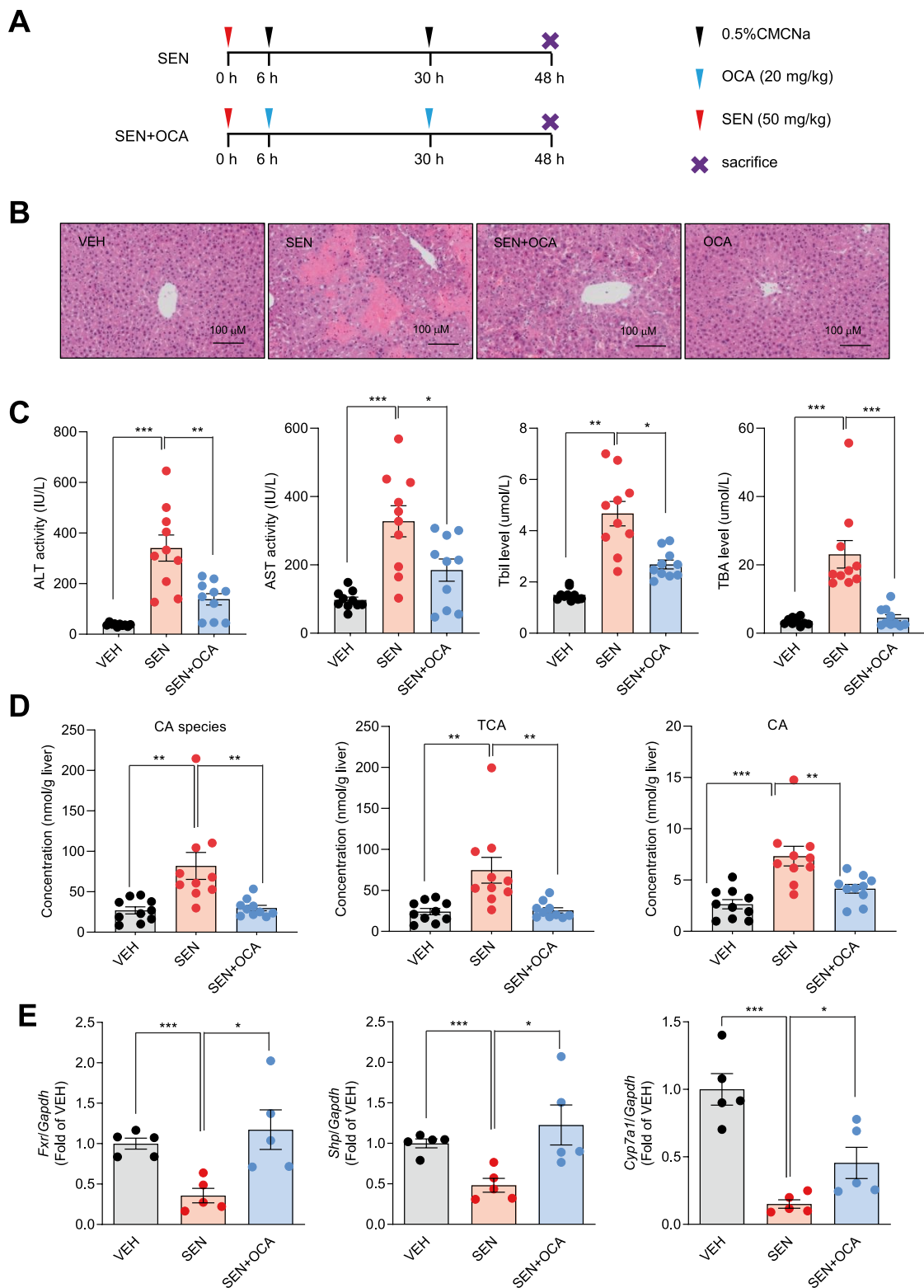


Fig. 7 The FXR agonist OCA confers a therapeutic effect against senecionine-induced HSOS in mice. **A** Mice were orally administered twice with OCA (20 mg/kg) at 6 and 30 h after senecionine exposure (50 mg/kg) and sacrificed at 48 h after senecionine exposure. **B** Typical images of HE staining. **C** Serum ALT, AST, TBA,

and Tbil level. **D** Levels of total and individual CAs in dissected liver tissues. **E** Hepatic mRNA expression of *Fxr*, *Shp*, and *Cyp7a1*. Values are expressed as the mean \pm SEM. * $p < 0.05$, ** $p < 0.01$, *** $p < 0.001$

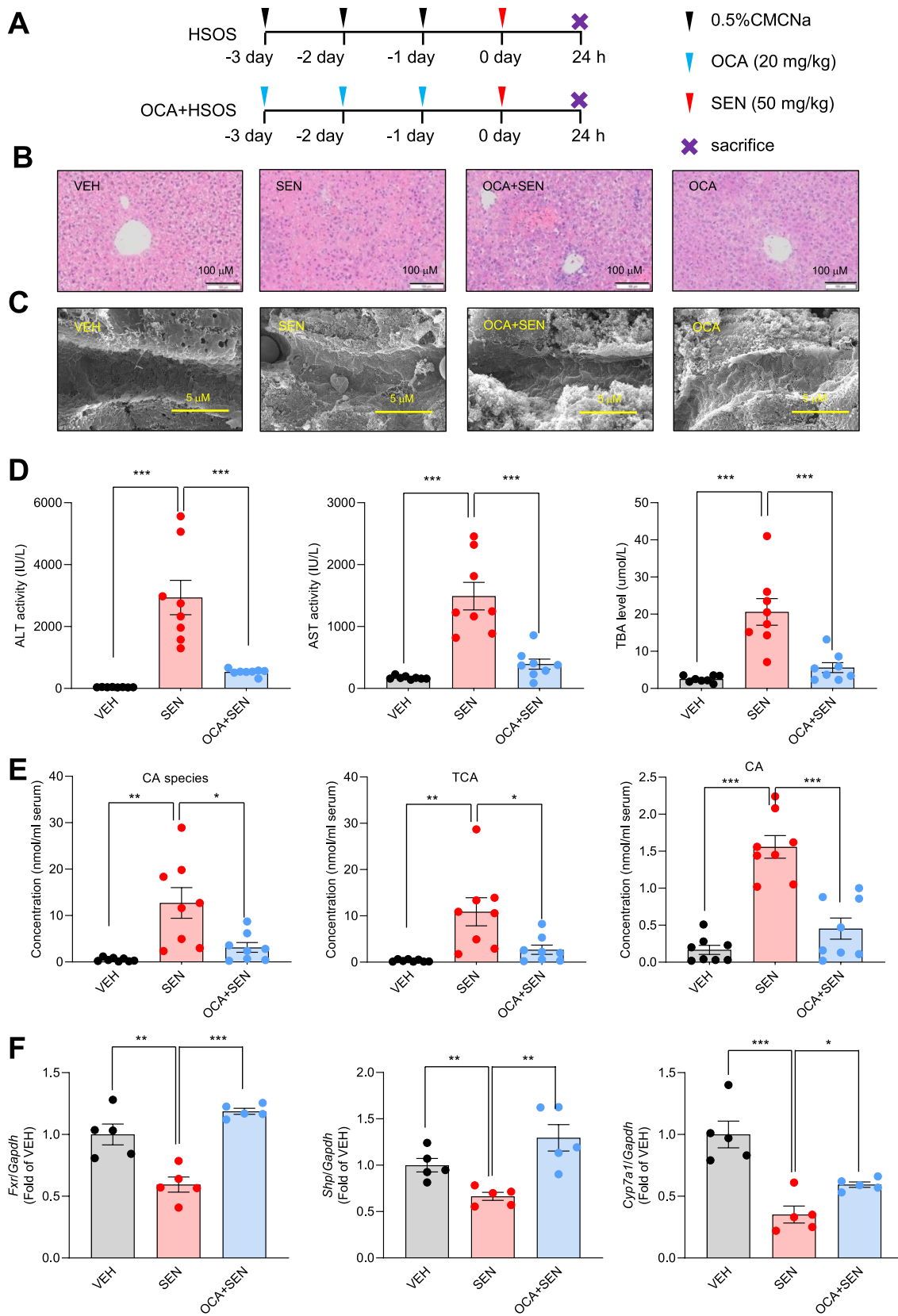


Fig. 8 OCA confers a prophylactic effect against senecionine-induced HSOS in mice. **A** Mice were pretreated with OCA (20 mg/kg) for 3 successive days, followed by a single exposure of senecionine (50 mg/kg) and sacrificed at 24 h after senecionine exposure. **B** Typical images of HE staining and SEM of dissected liver tissues. **C** Serum ALT, AST, and TBA level. **D** Total and individual CA species in serum. **E** Hepatic mRNA expression of *Fxr*, *Shp*, and *Cyp7a1*. Values are expressed as the mean \pm SEM. * $p < 0.05$, ** $p < 0.01$, *** $p < 0.001$

function as altered by PA exposure. Genomics studies by our group (Xiong et al. 2014) and others (Waizenegger et al. 2021; Hessel-Pras et al. 2020) further suggested impaired expression of several genes involved in bile acid biosynthesis in rodents and human HepaRG cells. Bile acid synthesis begins with the formation of 7α -hydroxycholesterol by CYP7A1, leading to the formation of the two primary bile acids CA and chenodeoxycholic acid (Russell 2003). CA biosynthesis involves an additional hydroxyl group at steroid ring position 12, catalyzed by CYP8B1 (Li-Hawkins et al. 2002). Bile acids such as chenodeoxycholic acid, deoxycholic acid, and lithocholic acid can promote the interaction between FXR ligand-binding domain and steroid receptor coactivator-1 or LXXLL peptides with other nuclear receptors (such as LXR α and RXR α) (Makishima et al. 1999; Parks et al. 1999), where L is leucine and X is any amino acid. When bound to bile acids, FXR suppresses the transcription of the genes encoding CYP7A1 and CYP8B1, and promotes the transcription of the genes for the hepatic efflux transporters BSEP, MRP2 (Wang et al. 2008), thus preventing accumulation of cytotoxic bile acids within hepatocytes under normal conditions.

Our fluorescence immunostaining experiments in the present study showed decreased FXR protein levels in liver tissues from diagnostic biopsies and surgical specimens of PA-HSOS patients. FXR is highly expressed in the liver and ileum. Primary bile acid biosynthesis can be regulated by a hepatic FXR/SHP cascade or an ileum FXR/fibroblast growth factor 19/15 (FGF19 in human and FGF15 in murine) cascade (Song et al. 2009; Inagaki et al. 2005; Goodwin et al. 2000). In murine senecionine-induced HSOS, the hepatic FXR/SHP cascade was inhibited yet the ileum FXR/FGF15 cascade was not obviously affected. The fact that *Fxr*^{-/-} mice have aggregated liver injury during senecionine-induced HSOS suggest that FXR may protect against PA-HSOS. Consistent with the idea of a protective effect of FXR against PA-HSOS, treatment of mice with the FXR agonist OCA showed a therapeutic effect in senecionine-induced HSOS; OCA pretreatment also protected mice against developing HSOS upon senecionine exposure. And OCA reduced the increased CA species levels in serum to normal levels. Sinusoidal injury happens at the beginning of HSOS and distinguishes HSOS from other DILI (DeLeve et al. 1999 and 2003). FXR agonists

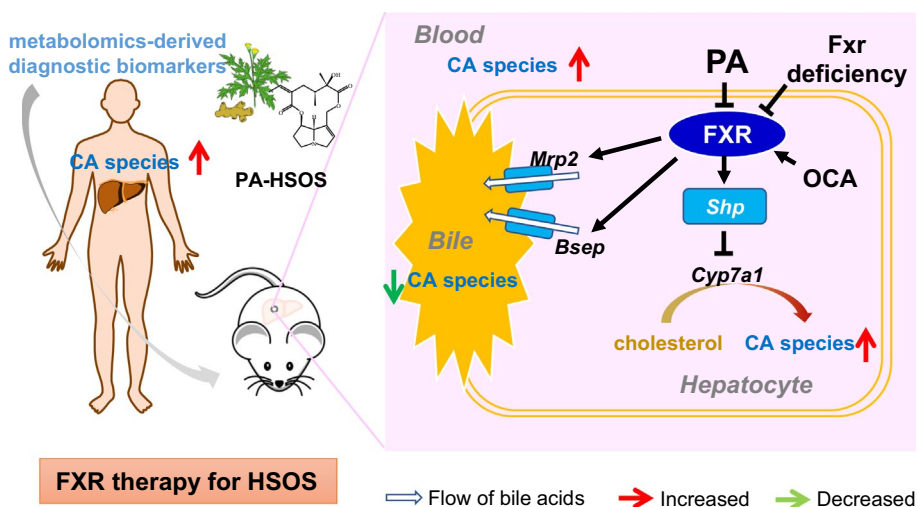
can inhibit sinusoidal remodeling and decreased portal pressure both in non-cirrhotic and cirrhotic hypertension (Schwabl et al. 2017; Verbeke et al. 2014). In present study, OCA was found to protect mice from senecionine-induced sinusoidal injury, specifically reducing damage to fenestration on the sieve plate. Taken together, the present study suggests a possible therapeutic intervention of PA-HSOS based on OCA-mediated activation of FXR.

The study has limitations. First, it is a single-centered retrospective study. Results from the discovery cohort were validated using a dependent cohort containing age- and sex-matched patients with PA-HSOS. However, the diagnostic performance of CA species in PA-HSOS needs to be further warranted by large multiple-center prospective studies. Second, the association of altered CA species with the severity of PA-HSOS cannot be predicted because of the unmatched sample size of patients with different severity grades (i.e., 66.7%, 16.7%, 3.3%, and 13.3% of PA-HSOS patient were graded as mild, moderate, severe, and very severe, respectively). Instead, we found CA species have good ability in differentiating those PA-HSOS patients likely to be responsive to therapy. Thirdly, the disorder of cholic acid species in the pathogenesis of PA-HSOS has not been elucidated. Elevated levels of individual CA, TCA, and GCA have been identified other DILI. A recent study (Ghallab et al. 2022) found increased TCA in APAP overdose and the interruption of bile acid re-uptake by pharmacological NTCP blockage and Oatp knockout strongly reduced APAP-induced hepatotoxicity. In our present study, we observed that inhibition of bile acid biosynthesis by pharmacological FXR activation (using OCA) reduced senecionine-induced hepatotoxicity in mice while and *Fxr* knockout strongly aggregates the injury. Our ongoing project will focus on illustrating the essential role of CA species in the pathogenesis of PA-HSOS.

In conclusion, PA-HSOS patients display significantly increased levels of CA species in serum. The results from our discovery cohort of 30 PA-HSOS patients were validated using a second cohort containing age- and sex-matched PA-HSOS patients. Serum levels of CA species were positively correlated with a conventional clinical indicator for PA-HSOS (Tbil) and showed excellent diagnosis ability for PA-HSOS. Levels of CA species also showed good ability in differentiating likely therapy-responsive PA-HSOS patients. Studies in a murine HSOS model induced by senecionine suggested that PAs may increase the biosynthesis of CA species by promoting *CYP7A1* and *CYP8B1* transcription via inhibition of the hepatic FXR-SHP cascade, and suggest a possible therapeutic intervention for treating PA-HSOS based on FXR agonists such as OCA.

Supplementary Information The online version contains supplementary material available at <https://doi.org/10.1007/s00204-024-03762-x>.

Fig. 9 Proposed model for the contribution of FXR-mediated bile acid homeostasis in PA-HSOS. Patients with PA-HSOS show increased serum level of CA species and decreased hepatic expression of FXR. In hepatocytes, senecionine inhibits Fxr and its downstream genes to promote bile acids synthesis and reduce bile acids secretion. Genetic knockout of Fxr enhances senecionine-induced liver damage. Pharmacological activation of Fxr rescues mice from senecionine-induced liver injury and recovers levels of CA species



Author's contributions Aizhen Xiong, Lili Ding, Zhengtao Wang, and Li Yang for study conception and design; Aizhen Xiong, Longhui Lu, Kaiyuan Jiang, Xiaoning Wang, Yan Chen, Wei Zhang, Qi Liao, Fan Yang, Yuzheng Zhuge, and Ping Liu participant screening and collection; Aizhen Xiong, Xiaoning Wang, and Lujin Li for statistical analysis and interpretation of data; Aizhen Xiong and Lili Ding for drafting of the manuscript; Wendong Huang, Fan Yang, Li Yang, and Zhengtao Wang for manuscript review and critical revision; Aizhen Xiong, Lili Ding, Zhengtao Wang, and Li Yang for obtaining funding.

Funding This work was funded by grants from the National Natural Science Foundation of China (No. 81603384 and 82122074), the Nature Science Foundation of Shanghai (No. 20ZR1473300, 23ZR1463200), Changjiang Scholars Programme of China (No. T2022255), the Shanghai Rising-Star Program (No. 17QA1403600), and the Shanghai Talents Development Foundation (No. 2020099).

Data availability The authors declare that the data supporting the findings of this study are available within the paper. All other data are available from the corresponding author upon reasonable request.

Code availability Not applicable.

Declarations

Conflict of interest The authors declare no competing interests.

Ethical approval Approved by Shanghai University of Traditional Chinese Medicine and Drum Tower Hospital of Nanjing.

Consent for publication All authors have agreed to publish this manuscript.

Consent to participate Not applicable.

References

Aubrecht J, Schomaker SJ, Amacher DE (2013) Emerging hepatotoxicity biomarkers and their potential to improve understanding and management of drug-induced liver injury. *Genome Med* 5(9):85

Beger RD, Dunn WB, Bandukwala A, Bethan B, Broadhurst D, Clish CB, Dasari S, Derr L, Evans A, Fischer S, Flynn T, Hartung

T, Herrington D, Higashi R, Hsu PC, Jones C, Kachman M, Karuso H, Kruppa G, Lippa K, Maruvada P, Mosley J, Ntai I, O'Donovan C, Playdon M, Raftery D, Shaughnessy D, Souza A, Spaeder T, Spalholz B, Tayyari F, Ubhi B, Verma M, Walk T, Wilson I, Witkin K, Bearden DW, Zanetti KA (2019) Towards quality assurance and quality control in untargeted metabolomics studies. *Metabolomics* 15(1):4

Chalasanani NP, Maddur H, Russo MW, Wong RJ, Reddy KR (2021) Practice parameters committee of the american college of gastroenterology. ACG clinical guideline: diagnosis and management of idiosyncratic drug-induced liver injury. *Am J Gastroenterol* 116(5):878–898

Chen WH, Wei YR, Xiong AZ, Li YM, Guan H, Wang Q, Miao Q, Bian Z, Xiao X, Lian M, Zhang J, Li B, Cao Q, Fan Z, Zhang W, Qiu D, Fang J, Gershwin ME, Yang L, Tang RQ, Ma X (2020a) Comprehensive analysis of serum and fecal bile acid profiles and interaction with gut microbiota in Primary Biliary Cholangitis. *Clin Rev Allergy Immunol* 58(1):25–38

Chen Y, Xiong F, Wang WQ, Jiang KY, Ye XL, Deng G, Wang CH, Yang L, Xiong AZ, Wang ZT (2020b) The long persistence of pyrrolizidine alkaloid-derived pyrrole-protein adducts in vivo: kinetic study following multiple exposures of a pyrrolizidine alkaloid containing extract of *Gynura japonica*. *Toxicol Lett* 323:41–47

Chiang JY (2003) Bile acid regulation of hepatic physiology: III. Bile acids and nuclear receptors. *Am J Physiol Gastrointest Liver Physiol* 284(3):G349–G356

Danan G, Bénichou C (1993) Causality assessment of adverse reactions to drugs—I. A novel method based on the conclusions of international consensus meetings: Application to drug-induced liver injuries. *J Clin Epidemiol* 46:1323–1330

DeLeve LD, McCuskey RS, Wang X, Hu L, McCuskey MK, Epstein RB, Kanel GC (1999) Characterization of a reproducible rat model of hepatic veno-occlusive disease. *Hepatology* 29:1779–1791

DeLeve LD, Ito Y, Bethea NW, McCuskey MK, Wang X, McCuskey RS (2003) Embolization by sinusoidal lining cells obstructs the microcirculation in rat sinusoidal obstruction syndrome. *Am J Physiol Gastrointest Liver Physiol* 284:G1045–G1052

Ding LL, Zhang EY, Yang Q, Jin L, Sousa KM, Dong B, Wang Y, Tu J, Ma X, Tian J, Zhang H, Fang Z, Guan A, Zhang Y, Wang ZT, Moore DD, Yang L, Huang WD (2021) Vertical sleeve gastrectomy confers metabolic improvements by reducing intestinal

- bile acids and lipid absorption in mice. *Proc Natl Acad Sci U S A* 118:e2019388118
- Gao H, Ruan JQ, Chen J, Li N, Ke CQ, Ye Y, Lin G, Wang JY (2015) Blood pyrrole-protein adducts as a diagnostic and prognostic index in pyrrolizidine alkaloid-hepatic sinusoidal obstruction syndrome. *Drug Des Devel Ther* 9:4861–4868
- Ghallab A, Hassan R, Hofmann U, Friebel A, Hobloss Z, Brackhagen L, Begher-Tibbe B, Myllys M, Reinders J, Overbeck N, Sezgin S, Zühlke S, Seddek AL, Murad W, Brecklinghaus T, Kappenberg F, Rahnenführer J, González D, Goldring C, Copple IM, Marchan R, Longerich T, Vucur M, Luedde T, Urban S, Canbay A, Schreiter T, Trauner M, Akakpo JY, Olyae M, Curry SC, Sowa JP, Jaeschke H, Hoehme S, Hengstler JG (2022) Interruption of bile acid uptake by hepatocytes after acetaminophen overdose ameliorates hepatotoxicity. *J Hepatol* 77(1):71–83
- Goodwin B, Jones SA, Price RR, Watson MA, McKee DD, Moore LB, Galardi C, Wilson JG, Lewis MC, Roth ME, Maloney PR, Willson TM, Kliewei SA (2000) A regulatory cascade of the nuclear receptors FXR, SHP-1, and LRH-1 represses bile acid biosynthesis. *Mol Cell* 6:517–526
- He Y, Ma J, Fan X, Ding L, Ding X, Zhang QY, Lin G (2021) The key role of gut-liver axis in pyrrolizidine alkaloid-induced hepatotoxicity and enterotoxicity. *Acta Pharm Sin B* 11(12):3820–3835
- Hessel-Pras S, Braeuning A, Guenther G, Adawy A, Enge AM, Ebmeyer J, Henderson CJ, Hengstler JG, Lampen A, Reif R (2020) The pyrrolizidine alkaloid senecionine induces CYP-dependent destruction of sinusoidal endothelial cells and cholestasis in mice. *Arch Toxicol* 94:219–229
- Hoofnagle JH, Björnsson ES (2019) Drug-induced liver injury—types and phenotypes. *N Engl J Med* 381:264–273
- Huang ZL, Jing X, Sheng Y, Zhang J, Hao Z, Wang ZT, Ji LL (2019) (-)-Epicatechin attenuates hepatic sinusoidal obstruction syndrome by inhibiting liver oxidative and inflammatory injury. *Redox Biol* 22:101117
- Inagaki T, Choi M, Moschetta A, Peng L, Cummins CL, McDonald JG, Luo G, Jones SA, Goodwin B, Richardson JA, Gerard RD, Repa JJ, Mangelsdorf DJ, Kliewer SA (2005) Fibroblast growth factor 15 functions as an enterohepatic signal to regulate bile acid homeostasis. *Cell Metab* 2:217–225
- IPCS; International Programme on Chemical Safety (1988) Environmental health criteria 80: pyrrolizidine alkaloids. World Health Organization, Geneva
- Jones RJ, Lee KS, Beschoner WE, Vogel VG, Grochow LB, Braine HG, Vogelsang GB, Sensenbrenner LL, Santos GW, Saral R (1987) Venooclusive disease of the liver following bone marrow transplantation. *Transplantation* 44:778–783
- Lee FY, de Aguiar Vallim TQ, Chong HK, Zhang Y, Liu Y, Jones SA, Osborne TF, Edwards PA (2010) Activation of the farnesoid X receptor provides protection against acetaminophen-induced hepatic toxicity. *Mol Endocrinol* 24:1626–1636
- Li-Hawkins J, Gåfvels M, Olin M, Lund EG, Andersson U, Schuster G, Björkhem I, Russell DW, Eggertsen G (2002) Cholic acid mediates negative feedback regulation of bile acid synthesis in mice. *J Clin Invest* 110:1191–1200
- Lin G, Wang JY, Li N, Li M, Gao H, Ji Y, Zhang F, Wang H, Zhou Y, Ye Y, Xu HX, Zheng J (2011) Hepatic sinusoidal obstruction syndrome associated with consumption of *Gynura segetum*. *J Hepatology* 54(4):666–673
- Makishima M, Okamoto AY, Repa JJ, Tu H, Learned RM, Luk A, Hull MV, Lustig KD, Mangelsdorf DJ, Shan B (1999) Identification of a nuclear receptor for bile acids. *Science* 284:1362–1365
- McDonald GB, Sharma P, Matthews DE, Shulman HM, Thomas ED (1984) Venocclusive disease of the liver after bone marrow transplantation: diagnosis, incidence, and predisposing factors. *Hepatology* 4:116–122
- Mendel VE, Witt MR, Gitchell BS, Gribble DN, Rogers QR, Segall HJ, Knight HD (1988) Pyrrolizidine alkaloid-induced liver disease in horses: an early diagnosis. *Am J Vet Res* 49:572–578
- Mohty M, Malard F, Abecassis M, Aerts E, Alaskar AS, Aljurf M, Arat M, Bader P, Baron F, Bazarbachi A, Blaise D, Ciceri F, Corbacioglu S, Dalle JH, Dignan F, Fukuda T, Huynh A, Masszi T, Michallet M, Nagler A, NiChonghaile M, Okamoto S, Pagliuca A, Peters C, Petersen FB, Richardson PG, Ruutu T, Savani BN, Wallhult E, Yakoub-Agha I, Duarte RF, Carreras E (2016) Revised diagnosis and severity criteria for sinusoidal obstruction syndrome/venoocclusive disease in adult patients: a new classification from the European Society for Blood and Marrow Transplantation. *Bone Marrow Transplant* 51:906–912
- Myant NB, Mitropoulos KA (1977) Cholesterol 7 alpha-hydroxylase. *J Lipid Res* 18(2):135–153
- Nevens F, Andreone P, Mazzella G, Strasser SI, Bowlus C, Invernizzi P, Drenth JP, Pockros PJ, Regula J, Beuers U, Trauner M, Jones DE, Floreani A, Hohenester S, Luketic V, Shiffman M, van Erpecum KJ, Vargas V, Vincent C, Hirschfield GM, Shah H, Hansen B, Lindor KD, Marschall HU, Kowdley KV, Hooshmand-Rad R, Marmon T, Sheeron S, Pencek R, MacConell L, Pruzanski M, Shapiro D, POISE Study Group (2016) A placebo-controlled trial of obeticholic acid in primary biliary cholangitis. *N Engl J Med* 375:631–643
- Pang X, Tang C, Cao P, Zhou L, Chen X (2021) Metabolic activation of retrorsine may disrupt bile acid homeostasis in mice through the Nrf2 pathway. *Curr Drug Metab* 22(11):870–881
- Parks DJ, Blanchard SG, Bledsoe RK, Chandra G, Consler TG, Kliewer SA, Stimmel JB, Willson TM, Zavacki AM, Moore DD, Lehmann JM (1999) Bile acids: Natural ligands for an orphan nuclear receptor. *Science* 284:1365–1368
- Pellicciari R, Fiorucci S, Camaioni E, Clerici C, Costantino G, Maloney PR, Morelli A, Parks DJ, Willson TM (2002) 6 α -Ethylchenodeoxycholic acid (6-ECDCA), a potent and selective FXR agonist endowed with anticholestatic activity. *J Med Chem* 45:3569–3572
- Russell DW (2003) The enzymes, regulation, and genetics of bile acid synthesis. *Annu Rev Biochem* 72:137–174
- Sang C, Wang X, Zhou K, Sun T, Bian H, Gao X, Wang Y, Zhang H, Jia W, Liu P, Xie G, Chen T (2021) Bile acid profiles are distinct among patients with different etiologies of chronic liver disease. *J Proteome Res* 20(5):2340–2351
- Schadt HS, Wolf A, Pognan F, Chibout SD, Merz M, Kullak-Ublick GA (2016) Bile acids in drug induced liver injury: Key players and surrogate markers. *Clin Res Hepatol Gastroenterol* 40(3):257–266
- Schwabl P, Hambruch E, Seeland BA, Hayden H, Wagner M, Garnys L, Strobel B, Schubert TL, Riedl F, Mitteregger D, Burnet M, Starlinger P, Oberhuber G, Deuschle U, Rohr-Udilova N, Podesser BK, Peck-Radosavljevic M, Reiberger T, Kremoser C, Trauner M (2017) The FXR agonist PX20606 ameliorates portal hypertension by targeting vascular remodeling and sinusoidal dysfunction. *J Hepatol* 66(4):724–733
- Shang H, Bai T, Zhu S, Yang X, Liu C, Xu D, Zhuge Y, Song Y, Hou X (2021) Prognostic factors for pyrrolizidine alkaloid-induced hepatic sinusoidal obstruction syndrome: a multicenter study in China. *Ann Transl Med* 9:11
- Song KH, Li T, Owsley E, Strom S, Chiang JY (2009) Bile acids activate fibroblast growth factor 19 signaling in human hepatocytes to inhibit cholesterol 7 alpha-hydroxylase gene expression. *Hepatology* 49:297–305
- Sutherland RJ, Deol HS, Hood PJ (1992) Changes in plasma bile acids, plasma amino acids, and hepatic enzyme pools as indices of functional impairment in liver-damaged sheep. *Vet Clin Pathol* 21:51–56
- Tian Q, Yang R, Wang Y, Liu J, Wee A, Saxena R, Wang L, Li M, Liu L, Shan S, Kong Y, Ma H, Ou X, You H, Zhao X, Jia J (2021) A

- high serum level of taurocholic acid is correlated with the severity and resolution of drug-induced liver injury. *Clin Gastroenterol Hepatol* 19(5):1009–1019
- Verbeke L, Farre R, Trebicka J, Komuta M, Roskams T, Klein S, Elst IV, Windmolders P, Vanuysel T, Nevens F, Laleman W (2014) Obeticholic acid, a farnesoid X receptor agonist, improves portal hypertension by two distinct pathways in cirrhotic rats. *Hepatology* 59:2286–2298
- Waizenegger J, Glück J, Henricsson M, Luckert C, Braeuning A, Hessel-Pras S (2021) Pyrrolizidine alkaloids disturb bile acid homeostasis in the human hepatoma cell line HepaRG. *Foods* 10(1):161
- Wang YD, Chen WD, Moore DD, Huang WD (2008) FXR: a metabolic regulator and cell protector. *Cell Res* 18:1087–1095
- Wang Y, Qiao D, Li Y, Xu F (2018) Risk factors for hepatic veno-occlusive disease caused by *Gynura segetum*: A retrospective study. *BMC Gastroenterol* 18:156
- Wang WQ, Chen Y, Yin Y, Wang XJ, Ye XL, Jiang KY, Zhang Y, Zhang JW, Zhang W, Zhuge YZ, Chen L, Peng C, Xiong AZ, Yang L, Wang ZT (2022a) A TMT-based shotgun proteomics uncovers overexpression of thrombospondin 1 as a contributor in pyrrolizidine alkaloid-induced hepatic sinusoidal obstruction syndrome. *Arch Toxicol* 96(7):2003–2019
- Wang Z, Ma J, He Y, Miu KK, Yao S, Tang C, Ye Y, Lin G (2022b) Nr2f-mediated liver protection by 18 β -glycyrrhetic acid against pyrrolizidine alkaloid-induced toxicity through PI3K/Akt/GSK3 β pathway. *Phytomedicine* 102:154162
- Wei J, Chen T, Liu YM, Sun S, Yuan Z, Zhang Y, Xiong AZ, Li LN, Wang ZT, Yang L (2023) Targeted bile acids metabolomics in cholesterol gallbladder polyps and gallstones: From analytical method development towards application to clinical samples. *J Pharm Anal* 13(9):1080–1087
- Willmot FC, Robertson GW (1920) *Senecio disease*, or cirrhosis of the liver due to *Senecio* poisoning. *Lancet* 196:848–849
- Woolbright BL, McGill MR, Staggs VS, Winefield RD, Gholami P, Olyae M, Sharpe MR, Curry SC, Lee WM, Jaeschke H, Acute Liver Failure Study Group (2014) Glycodeoxycholic acid levels as prognostic biomarker in acetaminophen-induced acute liver failure patients. *Toxicol Sci* 142:436–444
- Xiong AZ, Yang F, Fang L, Yang L, He Y, Wan YJ, Xu Y, Qi M, Wang X, Yu K, Tsim KW, Wang ZT (2014) Metabolomic and genomic evidence for compromised bile acid homeostasis by senecionine, a hepatotoxic pyrrolizidine alkaloid. *Chem Res Toxicol* 27:775–786
- Xiong AZ, Shao YL, Fang L, Yang X, Zhang S, Zheng J, Ding W, Yang L, Wang ZT (2019) Comparative analysis of toxic components in different medicinal parts of *Gynura japonica* and its toxicity assessment on mice. *Phytomedicine* 54:77–88
- Xiong H, Zhang C, Han L, Xu T, Saeed K, Han J, Liu J, Klaassen CD, Gonzalez FJ, Lu Y, Zhang Y (2022) Suppressed farnesoid X receptor by iron overload in mice and humans potentiates iron-induced hepatotoxicity. *Hepatology* 76(2):387–403
- Yamazaki M, Miyake M, Sato H, Masutomi N, Tsutsui N, Adam KP, Alexander DC, Lawton KA, Milburn MV, Ryals JA, Wulff JE, Guo L (2013) Perturbation of bile acid homeostasis is an early pathogenesis event of drug induced liver injury in rats. *Toxicol Appl Pharmacol* 268:79–89
- Yan T, Yan N, Wang H, Yagai T, Luo Y, Takahashi S, Zhao M, Krausz KW, Wang G, Hao H, Gonzalez FJ (2021) FXR-deoxycholic acid-TNF- α axis modulates acetaminophen-induced hepatotoxicity. *Toxicol Sci* 181(2):273–284
- Yang F, Huang X, Yi T, Yen Y, Moore DD, Huang WD (2007) Spontaneous development of liver tumors in the absence of the bile acid receptor farnesoid X receptor. *Cancer Res* 67:863–867
- Yang L, Xiong AZ, He YQ, Wang ZY, Wang CH, Wang ZT, Li W, Yang L, Hu ZB (2008) Bile acids metabolomic study on the CCl₄- and alpha-naphthylisothiocyanate-induced animal models: Quantitative analysis of 22 bile acids by ultraperformance liquid chromatography-mass spectrometry. *Chem Res Toxicol* 21:2280–2288
- Yang F, Tang X, Ding L, Zhou Y, Yang Q, Gong J, Wang G, Wang Z, Yang L (2016) Curcumin protects ANIT-induced cholestasis through signaling pathway of FXR-regulated bile acid and inflammation. *Sci Rep* 6:33052
- Yang X, Wang H, Ni HM, Xiong AZ, Wang ZT, Sesaki H, Ding WX, Yang L (2017) Inhibition of Drp1 protects against senecionine-induced mitochondria-mediated apoptosis in primary hepatocytes and in mice. *Redox Biol* 12:264–273
- Zhang L, Wei TT, Li Y, Li J, Fan Y, Huang FQ, Cai YY, Ma G, Liu JF, Chen QQ, Wang SL, Li H, Aloga RN, Liu B, Zhao DS, Shen JH, Wang XM, Zhu W, Li P, Qi LW (2018) Functional metabolomics characterizes a key role for *N*-acetylneuraminic acid in coronary artery diseases. *Circulation* 137:1374–1390
- Zhang W, Liu L, Zhang M, Zhang F, Peng C, Zhang B, Chen J, Li L, He J, Xiao J, Feng Y, Wang X, Xiong A, Yang L, Zou X, Yu Y, Zhuge YZ (2021) Validation of the Nanjing Criteria for diagnosing pyrrolizidine alkaloids-induced hepatic sinusoidal obstruction syndrome. *J Clin Transl Hepatol* 9:345–352
- Zhu L, Zhang CY, Li DP, Chen HB, Ma J, Gao H, Ye Y, Wang JY, Fu PP, Lin G (2021) Tu-San-Qi (*Gynura japonica*): the culprit behind pyrrolizidine alkaloid-induced liver injury in China. *Acta Pharmacol Sin* 42(8):1212–1222
- Zhuce YZ, Wang Y, Zhang F, Zhu CK, Zhang W, Zhang M, He Q, Yang J, He J, Chen J, Zou XP (2018) Clinical characteristics and treatment of pyrrolizidine alkaloid-related hepatic vein occlusive disease. *Liver Int* 38:1867–1874
- Zhuce YZ, Liu Y, Xie W, Zou X, Xu J, Wang J (2019) Chinese society of gastroenterology committee of hepatobiliary disease. Expert consensus on the clinical management of pyrrolizidine alkaloid-induced hepatic sinusoidal obstruction syndrome. *J Gastroenterol Hepatol* 34:634–642

Publisher's Note Springer Nature remains neutral with regard to jurisdictional claims in published maps and institutional affiliations.

Springer Nature or its licensor (e.g. a society or other partner) holds exclusive rights to this article under a publishing agreement with the author(s) or other rightsholder(s); author self-archiving of the accepted manuscript version of this article is solely governed by the terms of such publishing agreement and applicable law.